

EETA79001 – 7942 grams

A) Olivine-phyric Shergottite

B) Basaltic Shergottite

C) Entrapped Soil ?



Figure 1. Photograph of EETA79001 as it was found on the ice (NASA # S80-28838). Note fusion crust.

Introduction

EETA79001 is the largest stony meteorite returned by the 1979 ANSMET expedition (Cassidy and Rancitelli 1982). It was found on the ice at the Elephant Moraine location near Reckling Peak, Victoria Land, Antarctica (figure 1). This sample is especially important, because glass inclusions in it were found to contain rare-gas and nitrogen compositions and isotopic ratios matching those of the Martian atmosphere as determined by the Viking spacecraft (Bogard and Johnson 1983a; Becker and Pepin 1984; Ott and Begemann 1985b; Garrison and Bogard 1998), hence demonstrating the Martian origin for this class of meteorites (Hunten *et al.* 1987). EETA79001 is also important because it contains direct evidence for entrapment of highly irradiated Martian soil (Rao *et al.* 2011; Hidaka *et al.* 2009). *But this rock is complicated and this compiler fears he may not do it justice (who says we know how to “read a rock”?).*

EETA79001 is a unique shergottite (achondrite) containing two different igneous lithologies (labeled A and B) separated by an obvious, linear contact and also containing “pockets” and veinlets of dark glass, labeled lithology C (Reid and Score 1981). A photograph illustrating the contact between A and B appeared on the cover of EOS, January 1981 (figure 2), because this is the first meteorite found to contain a “geological contact” between two lithologies. Based on texture, lithology B is a basalt, whereas lithology A is a basaltic melt containing numerous inclusions of mafic minerals as xenocrysts (McSween and Jarosewich 1983; McSween 1985; Berkley *et al.* 1999, 2000; Shearer *et al.* 2008; Papike *et al.* 2009).

The report of the preliminary examination of EETA79001 (Score and Reid 1981) makes interesting reading in light of what has since been discovered (*see*

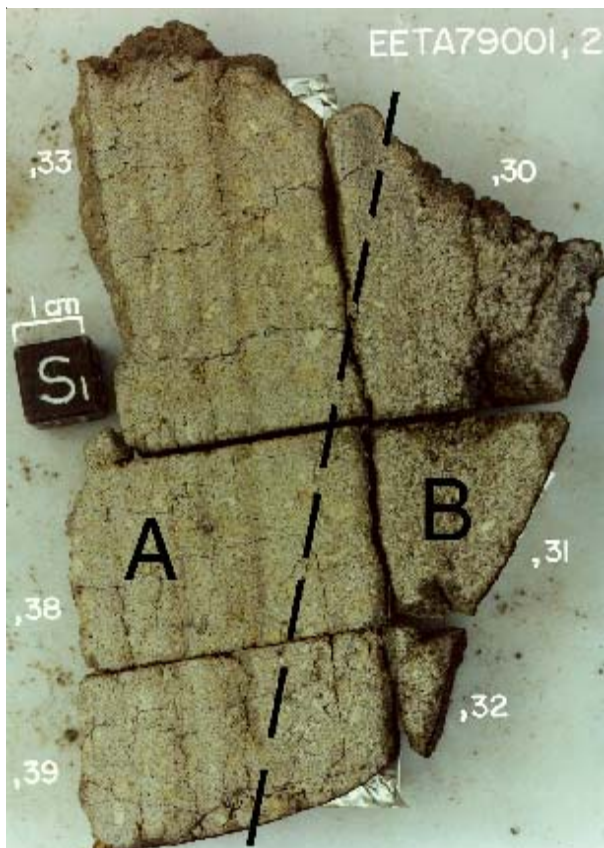


Figure 2. Photograph of interior slice of EETA79001 showing contact between lithology A and B. NASA photo # S81-25273. Cube is 1 cm.

below). “Several large, black fine-grained clasts as large as 2.5 cm are scattered over the cut face. Some of these black clasts contain vugs which have glass in their interior. Upon chipping one of these clasts, containing a vug, the entire clast popped out easily and no matrix adhered to the clast. Numerous veins of black material criss-cross each other. These veins run through a black clast. The longest vein is ~14 cm long.” “The dark clasts are apparently loci of melting; in many cases they connect with the thin black glassy (?) veinlets that traverse much of the meteorite.” These glass veins and black clasts have been loosely referred to as lithology C (see below).

It has proven difficult to determine the original igneous crystallization age of EETA79001 (see section on Radiogenic Isotopes), possibly because it contains a mixture of igneous source rocks, has been disturbed by multiple shock events or has incorporated old, irradiated Martian soil. It is about 170 m.y. old with 0.6 m.y. exposure to cosmic rays.

Wadhwa *et al.* (1994) presented a model for the origins

of the shergottites, including EETA79001, in which “their parent magmas were ultimately derived from partial melts of the partly depleted mantle of their parent planet, and acquired their distinct characteristics through processes such as crystal fractionation, crystal accumulation, magma mixing/assimilation, and crustal contamination.” On the other hand, Mittlefehldt *et al.* (1997, 1999) have argued that lithology A is an impact melt, which incorporates lithology B as a clast. In their mixing model using both major and trace elements, the composition of lithology A can be reasonably approximated as a simple mixture of 44% lithology B and 56% ALHA77005. Boctor *et al.* (1998) presented preliminary petrologic evidence in favor of an impact-melt origin. However, the evidence of mixing between basaltic lava with a significantly

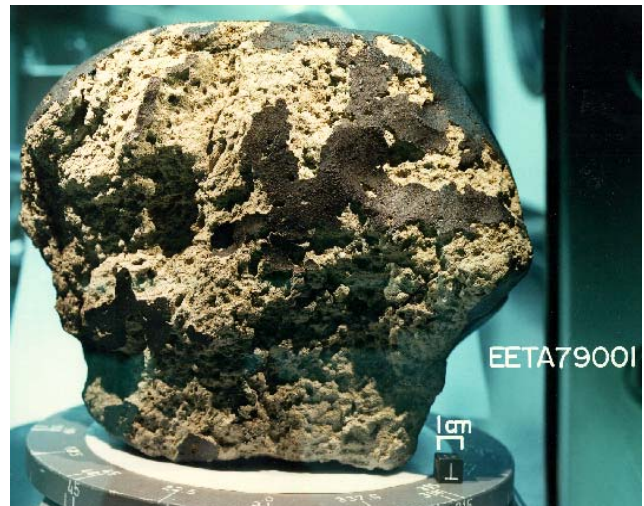


Figure 3. Photograph of top surface of EETA79001 illustrating partial coating with fusion crust. (NASA # S80-37480)



Figure 4. Photograph of west end of EETA79001 illustrating unusual “regmaglypt” and first saw cut. The dotted line is approximate location of the second cut. (NASA #S80-37630)

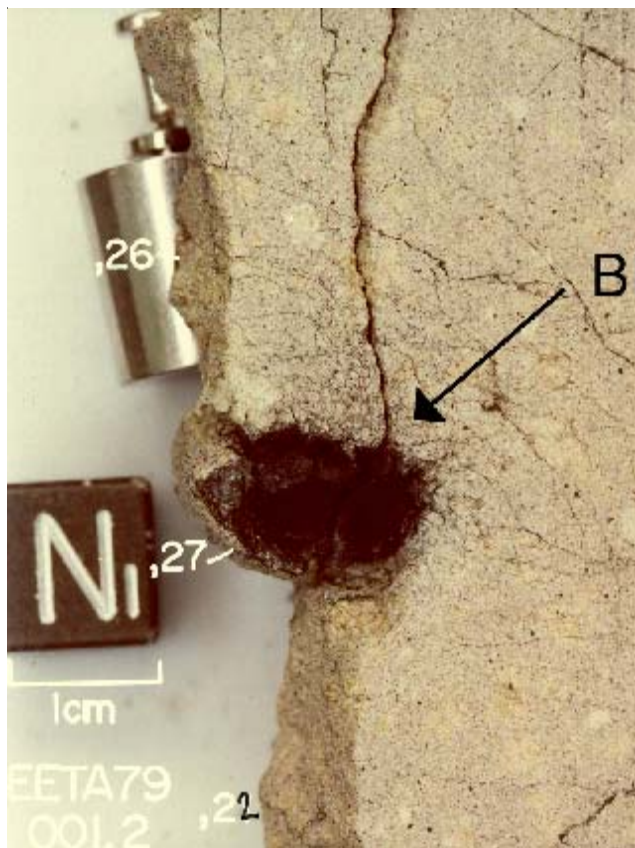


Figure 5. Close-up photo of a portion of slab EETA79001,22 illustrating mottled appearance of lithology A and “discovery” pod (,27) of glass and fine glass veins. Note the very large vesicle in the glass pod (BRAVO). Cube is 1 cm for scale. (NASA # S81-25242)

irradiated Martian regolith is a reasonable interpretation of the excess neutron capture records observed in EETA79001 and other Martian shergottites (Hidaka et al. 2009). The saw cut through the middle of EETA79001 seems to have caught this mixing process in action, and if this is the case, then this is significant to an understanding all Martian basalts.

Mineralogical Mode

	McSween and Jarosewich 1983			Schwandt <i>et al.</i> 2001			
	,75(A),68(A)	,79(A)	,80(A)	,79(B)	,71(B)	,69(B)	,68(A)
thin section				,80(B)			
	<i>volume %</i>						
pigeonite	62.8	60.7	54.5	54.4	32.2	31.8	42
augite	3.2	6.5	8.5	11.6	23.9	24.5	18
maskelynite	18.3	15.9	17.0	28.2	29.4	29.6	22
olivine	10.3	7.2	9.1				3
orthopyroxene	3.4	5.7	7.2				3
opaque	2.2	4.0	3.0	3.4	3.8	3.4	3
whitlockite	tr	tr	0.4	0.7	0.2	0.2	2
mesostasis		tr	0.3	1.1	0.5	0.5	

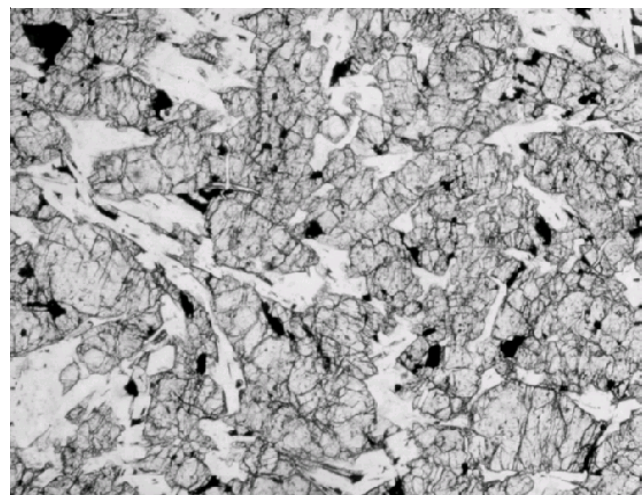


Figure 6. Photomicrograph of thin section of EETA79001,79 illustrating the fine-grained matrix of lithology A. Field of view is 2.2 mm.

So, EETA79001 is a most complex sample. In addition to the above lithologies, there are glass veins that are the result of shock melting, and there are weathering products (druse) along these veins.

Petrography

All surfaces of this meteorite are covered by at least some fusion crust, so that the sample represents a nearly complete piece. On the top surface, about half of the fusion crust is partially plucked away (figure 3). One end (W) has a deep “regmaglypt” that is covered with fusion crust (Score *et al.* 1982) (figure 4). The sample has many penetrating fractures — some lined with thin black glass and connected to interior glass pods. However, the sample was coherent enough to hold together during sawing.

At least 4 lithological features are found within EETA79001. While most of the rock is a fine-grained mix of pyroxene and maskelynite with small mafic inclusions (termed lithology A), there is a gradational



Figure 7. Close-up photo of sawn surface of EETA79001,30 illustrating the basaltic texture of lithology B. Cube is 1 cm. (NASA # S81-25238)

boundary to a sub-ophitic textured basalt (termed lithology B). The numerous examples of shock-melted glass and thin glass veins are termed lithology C (see below) and the small mafic inclusions appear to be another lithology (sometimes called lithology X). Lithology A is somewhat more mafic than lithology B (see table 1, figure 2).

Lithology A is made up of a basaltic host (pyroxene, maskelynite, high-Ti chromite, merrillite, minor Cl-apatite, ilmenite, pyrrhotite and mesostasis) containing apparently exotic crystals and clusters of olivine, Cr-spinel and low-Ca pyroxene) (figures 5,6). Lithology A is now termed an olivine-phyric Shergottite (Goodrich 2002). Papike et al. (2009) compare the various shergottites.

Lithology B is a homogeneous basalt containing augite laths in a matrix of pigeonite-augite, maskelynite, ulvöspinel-ilmenite intergrowth, whitlockite, Cl-apatite, and mesostasis (figure 7). Mineral compositions indicate an oxidation state similar to that of shergottites. The groundmass of lithology B has a slightly larger grain size (0.3 mm) than lithology A (0.15 mm). Overall, the basaltic texture of lithology B (figure 8) is similar to

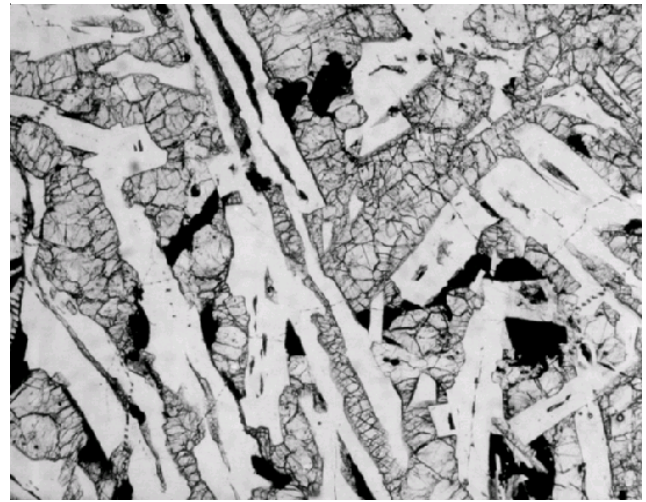


Figure 8. Photomicrograph of thin section of EETA79001,88 illustrating basaltic texture of lithology B. Field of view is 2.2mm.

that of Shergotty. However, lithology B is depleted in light rare-earth-element contents, when compared with other shergottites (see figure 15).

The mafic xenocrysts found in lithology A consist of light yellow, olivine/orthopyroxene clusters up to 3 mm in size that are evenly spread out throughout the lithology A. These are referred to as “ultramafic clusters” or “megacrysts” (McSween and Jarosewich, 1983) and as “lithology X” (Treiman 1995a). The compositions of the minerals in these xenocrysts are Mg-rich and similar to the corresponding phases in the poikilitic areas of ALHA77005 (Wadhwa *et al.* 1994). Wadhwa *et al.* observed that orthopyroxene xenocrysts were often rimmed by coronas of pigeonite having the same composition as that in the groundmass, and that xenocrysts of olivine had irregular embayments cutting across internal zoning patterns (figure 9). Berkley *et al.* (1999, 2000) carefully studied on particular mafic inclusion (X14, in section ,68) and tentatively concluded that the “Mg-rich orthopyroxene crystallized at some depth, followed by thermal annealing and incorporation into the EETA79001A magma”.

So, three working hypotheses need to be considered: 1) An igneous origin is argued by McSween and Jarosewich (1983) who conclude “Both lithologies probably formed from successive volcanic flows or multiple injections of magma into a small, shallow chamber”. However, the difference in initial Sr is proof that the two main lithologies (A and B) are not derived from the same source (*see section on Radiometric Isotopes*), 2) an alternative interpretation is that lithology

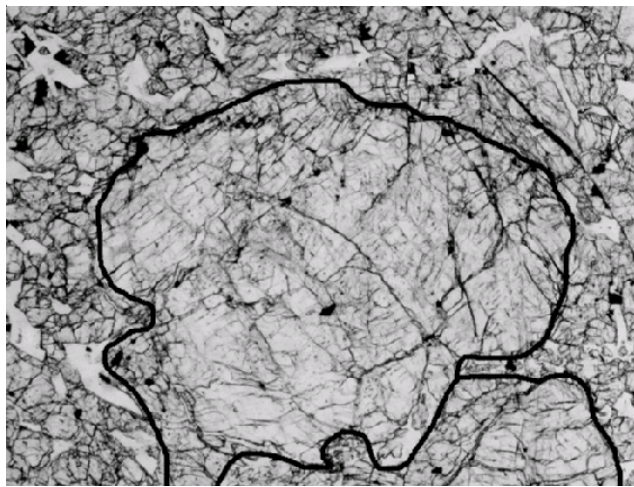


Figure 9. Photograph of thin section of EETA79001,79 illustrating a large olivine clast with irregular boundary in lithology A. Field of view is 2.2 mm.

A represents an impact melt rock that incorporates lithology B, and the ultramafic clusters, as clasts (Mittlefehldt *et al.* 1997, 1999), and **3**) EETA79001 is a lava flow that has been contaminated by soil erosion and entrapment as it flowed out over the ancient Martian regolith (see figure 38).

Key to understanding the origin of EETA79001, is the observation of a gradational contact between lithology A and B (Steele and Smith 1982b; McSween and Jarosewich 1983; Niekerk *et al.* 2007)(see figure 2). Is this contact a boundary between different lava flows, or is lithology B, instead, a clast in lithology A?

Lithology C is an assemblage of glass “pods” and thin, interconnecting, glass veins (Walton *et al.* 2010). Although lithology C has commonly been referred to as “glass,” it actually consists of finely intermingled vitreous and cryptocrystalline materials (McSween and Jarosewich 1983; Gooding and Muenow 1986; Rao *et al.* 1998). Martinez and Gooding (1986) describe the true glassy part as dark brown to black, whereas the microcrystalline components include both dark gray-brown phases and colorless to white phases (figure 10). Both large vugs and small vesicles are common features. Some dark colored phases (probably pyroxenes) display quench textures that suggest origins by incomplete crystallization of the melt of this unit. In contrast, the light-colored phases might be a mixture of incompletely melted relict grains and post-melting reaction products.

In 1983, Bogard and Johnson discovered high

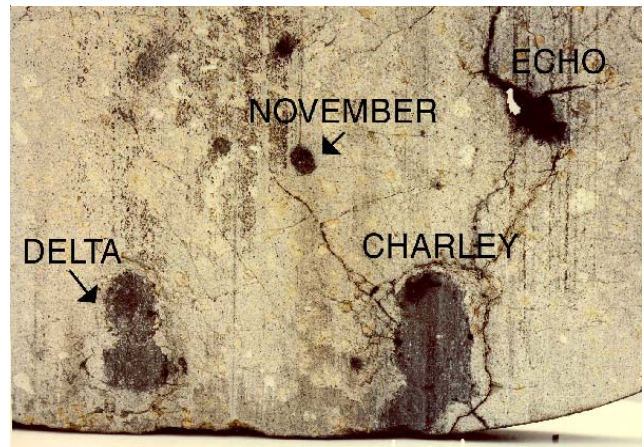


Figure 10. Close-up photograph of a portion of slab EETA79001,22 illustrating several of the largest glass “pods” and interconnecting glass veins along cracks in lithology A. (NASA # S81-25257)

concentrations of rare gases (Ar, Ne, Kr, Xe) in portions of lithology C (see section on Other Isotopes). Figure 5 illustrates the “discovery pod” (,27) which contains a large (0.8 mm) vug or vesicle. Altogether there are more than 20 glass “pods” exposed on the sawn surfaces of EETA79001, with ~ 5 large ones (~1 cm). Most are found in lithology A, but one (PAPA) was studied from lithology B. Table 1 lists these glass pods and gives them each a new name in order to more clearly distinguish them. When the rock was sawn and broken, some of these glass pods broke free from the basaltic matrix (,8 and ,27). Garrison and Bogard (1998) and Bogard and Garrison (1998) have now revised the

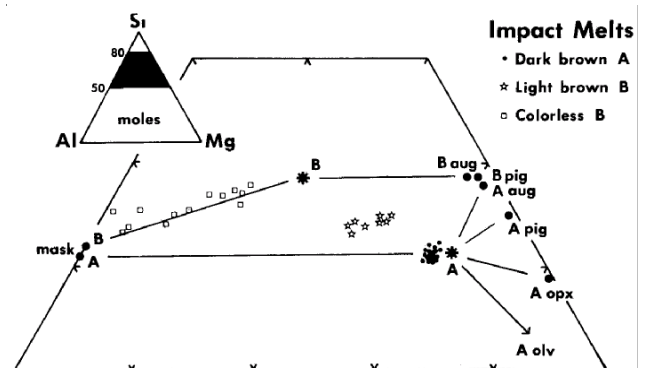


Figure 11. Composition diagram for glass in EETA79001. Stars A and B are bulk compositions of lithology A and B respectively. The dark brown glass has a composition like that of the host rock, while the light brown glass and colorless glasses are along the join with the composition of maskylynite. This is figure 5 in McSween and Jarosewich 1983, GCA 47, 1507.

Table 1. Glass pods (lithology C) and their locations in EETA79001.

(signal corps call letters)

ALPHA	- 8 mm, round, with vesicle - exposed by first saw cut on ,1 (figure S80-37631) - piece ,8 broke free from ,2 before slab was cut - portion (~1/2) remains on ,1 sawn surface - studied by Bogard and Garrison 1998 and Garrison and Bogard, 1998
BRAVO	- “discovery pod”, studied by Bogard, Pepin, Swindle - 1 cm, exposed by first sawcut on ,1 - large vug (7 mm) - 1/2 piece ,27 broke free, part remains on ,22 (becomes ,120 -,126) - Sr in ,27 by Nyquist (Sr 15.5 ppm) - piece ,26 (PB) contains thin glass veins associated with ,27 - pieces ,120 - ,126, inc. ,122 Swindle (Hohenberg)
CHARLEY	(1 x 2.5 cm) - exposed by first sawcut - microcrystalline - on ,1 and slab ,22 (did not extend thru slab ,22) - contained in piece ,216 (at edge of both saw cuts 1980 and 1986) - ,249 - ,257 from piece ,216 - closeup photo S81-25257 of Charley, Delta, Echo on slab ,22 - exposed to outer surface of rock and surrounded by penetrating cracks - Sr in ,186 by Nyquist (Sr 15 ppm)
DELTA	- (dumbell-shaped pod) exposed by first sawcut - microcrystalline - on ,1 and ,22 (did not extend thru slab ,22) - exposed again by 1986 cut through ,1 again exposed on ,312 - contained in piece ,216 (at edge of both saw cuts 1980 and 1986) - ,259 - ,263 from ,216 - cracks leading to outside surface S80-37631 - ,194 this half of glass “pod” was carefully lifted out of slab ,22 - “druse” salts studied by Gooding, Clayton, Wright (sample ,239) - S86-37533 shows large patch of “white druse” adjacent to black glass - black glass is surrounded by thick grey (altered) band in ,1 - minor orange “stain” seen in “white-druse” - Sr in ,195 studied by Nyquist (Sr = 15 ppm)
ECHO	- large glass-lined cavity - seen initially on first saw cut on ,1 and ,2 - complex shape along open fracture, portion on ,52 - extends through slab ,22 and on ,312 (derived from ,2) - ,54 ,56 ,57 derived from ,52 S81-25252, S90-34035 - penetrating cracks leading to CHARLEY and outer surface of rock - possibly connecting to “regmaglypt” on exterior surface - Sr in ,54 by Nyquist (17 ppm Sr) - TS,73 from PB,53 studied by Walton et al. 2010
FOXTROT	- 4 mm exposed on first cut S81-25268 S80-37631
GOLF	- 4 mm exposed by 1986 cut S86-26477
HOTEL	- 2 mm glass inclusion, near white inc. on ,38 - S81-25268 S81-25267
ITEM	- exposed by second saw cut from ,2 of backside of slab ,22 - 3 mm with 2 small vesicles exposed on ,312 - on edge of 312 after break during small saw cut - S81-25252
JULIET	- 3 mm with 2 mm vesicle - exposed on ,307 - S90-34035

LIMA	- small shiny black glass pod on ,309 - S90-34036
MIKE	- small pod exposed on ,311 and ,313 (exhibited by Smithsonian) - S90-34042 S90-34041
NOVEMBER	- small exposed by first saw cut ,1 and ,22 - ,197 studied by Nyquist (17 ppm Sr) - salts studied by Gooding
OSCAR	- small exposed first saw cut ,1 and ,22
PAPA	- Glass in lithology B - near outer surface, S81-25259 - ,188 (from ,43) studied by Nyquist (30 ppm Sr) - TS ,71 and ,72 (from ,47) include glass from PAPA - ,104 studied by Bogard and Garrison and Garrison and Bogard, 1998

note: it is a crying shame that these glass pods have not been properly studied !

composition of the Martian atmosphere based on their recent measurement of glass pod ,8. Nyquist *et al.* (1986) found that the I_{Sr} was significantly different for different “pods” (*see section on Radiogenic Isotopes*).

Thin black glass veins (~0.5 mm wide) extend from and connect various “pods” of black glass (Score *et al.* 1982; McSween and Jarosewich 1983; Rao *et al.* 1998). McSween and Jarosewich found the composition of the dark brown vesicular glass veins and pods included in lithology A was generally similar to the bulk composition of lithology A (figure 11) whereas, Rao *et al.* find that lithology C represents a mixture of ~85% lithology A, plus ~7% maskelynite and ~8% Martian soil. However, two different glasses have been found in lithology B. Non-vesicular, clear glass varies in composition from maskelynite to bulk B and light-brown glass found to have a composition intermediate between bulk A and B.

Martinez and Gooding (1986) describe the “white druse” commonly found associated with lithology C in the interior of EETA79001 (figure 12). Martinez and Gooding describe this material to consist of “*thin saccharoidal coatings and veins of a colorless to white, translucent phase of dull to resinous luster.*” Gooding and Muenow (1986), Wentworth and Gooding (1986), Gooding *et al.* (1988) and Gooding and Wentworth (1991b) have studied the mineralogical composition of this material. “White druse” material has also been found along rock fractures (*e.g.* piece ,312). Photo S90-34041 of ,313 (display sample) shows a large off-white patch (8 mm) that may be an additional deposit of “druse.” Gooding *et al.* (1988) showed that this material was mostly $CaCO_3$ (calcite), but also

included $CaSO_4$. Isotopic data on the “druse” is discussed in the section on “*Other Isotopes*”.

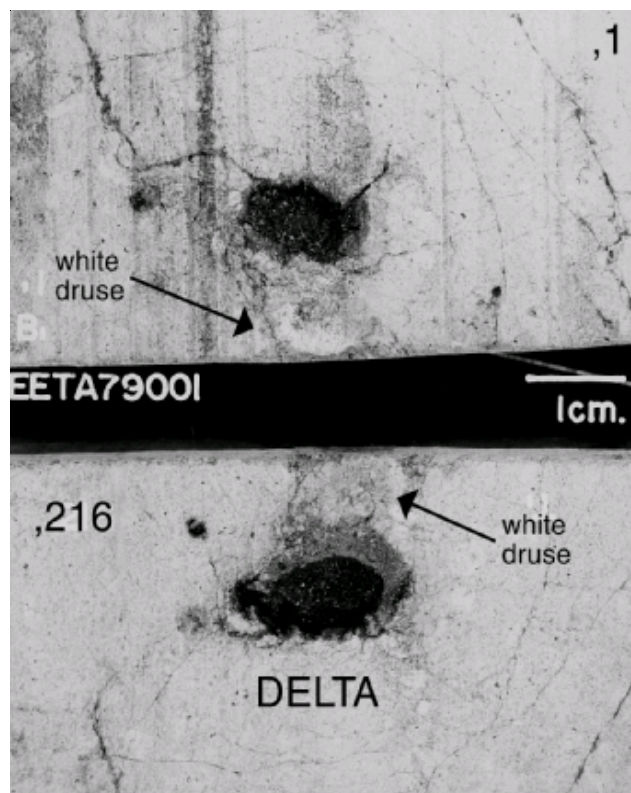


Figure 12. The saw cut that separated ,216 and ,1 exposed another glass pod “DELTA” in EETA79001. Note the concentric color changes in the glass. Adjacent to the glass was a large deposit of white carbonate “druse” (sample ,239). NASA photo # S86-37533

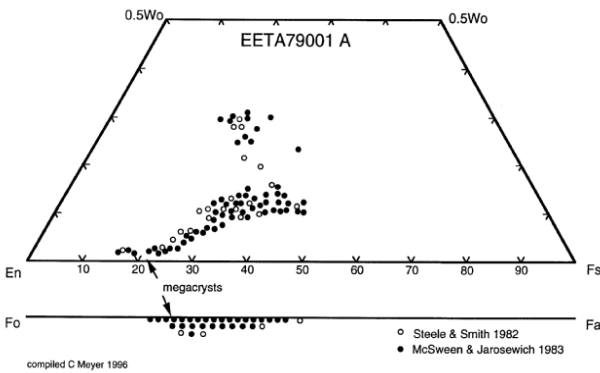


Figure 13. Composition diagram for pyroxene and olivine in EETA79001 lithology A. Note the data for the megacrysts in lithology A were the most magnesian.

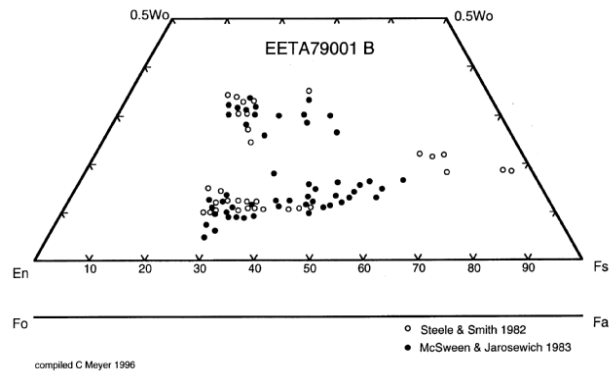


Figure 14. Composition diagram for pyroxene in EETA79001 lithology B. Note the pyroxene is zoned to Fe-rich.

Mineral Chemistry

Olivine: Olivine has a range of composition (Fo_{81-55}) in EETA79001 and contains a significant amount of NiO (~0.06%) (Steele and Smith 1982b). The Fe/Mg of olivine appears to be in equilibrium with coexisting pyroxene. The olivine in the “megacrysts” in lithology A is the most Mg-rich (McSween and Jarosewich 1983). Boctor *et al.* (1998) have reported evidence of high pressure phase transition and vitrification in olivine megacrysts from lithology A. Herd *et al.* (2001) have determined Ni, Co, Cr and V in olivine from Martian meteorites. Shearer *et al.* (2008) have also studied the more mafic olivines in shergottites.

Pyroxene: There is a range of pyroxene compositions in EETA79001 (Steele and Smith 1982b; McSween and Jarosewich 1983). Mg-rich orthopyroxene coexists with olivine in the “xenocryst clusters” in lithology A. In the groundmass of lithology A and B, zoned pigeonite and sub-calcic augite vary from Mg-rich to Fe-rich (figure 13 and 14). Wadhwa *et al.* (1994a) determined Y, Sc, Cr, Zr and Ti in the pyroxenes in EETA79001. McSween and Jarosewich, and Steele and Smith, reported pyroxferroite in the mesostasis of lithology B, but gave no analysis. Mikouchi *et al.* (1997, 1998) have studied the complex zoning of the pyroxenes in basaltic lithology B, EETA79001 and found the zoning in these pyroxenes to be similar to that of those in QUE94201.

Plagioclase: Maskelynite grains generally fill interstices between clinopyroxene crystals in both lithologies, consistent with the interpretation that plagioclase crystallized after pyroxene. Plagioclase is An_{65-50} in both lithologies. Treiman and Treado (1998)

have determined the Raman spectra of maskelynite in EETA79001.

Chromite: Chromite occurs as euhedral inclusions in the olivine in the “xenocryst clusters” in lithology A. Chromites are described as “two-phase” by Steele and Smith (1982b). One phase is low Ti, the other high Ti. “About one-fifteenth of the total iron in the Ti-poor chromites, and one-ninth of that in the Ti-rich chromites, was converted to ferric iron to satisfy stoichiometry, again confirming the oxidizing conditions.”

Amphibole: Treiman (1997d, 1998b) gives the composition of “kaersutitic” amphibole found in melt inclusions in pigeonite in EETA79001.

Ulvöspinel and Ilmenite: These oxides are found in the mesostasis of lithology B. Steele and Smith (1982b), report that “up to one-fifth of the iron was converted to ferric state.”

Ringwoodite (?) and Majorite (?) were tentatively reported in “shock veins” by Steele and Smith (1982b) and Boctor *et al.* (1998). These are high pressure polymorphs of olivine and pyroxene and would give an indication of the shock pressure reached by this meteorite, if they are confirmed.

Phosphate: Both whitlockite and Cl-apatite have been reported (Steele and Smith 1982b). Wadhwa *et al.* (1994a) determined the REE content of whitlockites in several shergottites and showed that they contained most of the REEs in these rocks.

Sulfide: Steele and Smith (1982b) reported pyrrhotite $\text{Fe}_{0.91}\text{S}$. McSween and Jarosewich (1983) reported Ni in the sulfides in lithology A, but not in B. They also reported pentlandite.

Carbonate: Calcium carbonate has been reported in the “white druse” (Gooding *et al.* 1988; Clayton and Mayeda 1988; Wright *et al.* 1988) related to glass pod DELTA (sample ,239). X-ray diffraction by Gooding *et al.* established that this material was largely calcite.

Other salts: Gooding (1992) summarized the various minor “salts,” including sulfates and phosphates, found in EETA79001 and other Martian meteorites. Gooding and Muenow (1986) reported a grain with Pb:Cr:S ~ 6:2:1, which Treiman (1999) interpreted as phoenicochroite-lanarite solid solution.

Glass: The composition of glass in EETA79001 has been reported in McSween and Jarosewich (1983). The glass pods and veins in lithology A generally have the composition of A and often contains secondary skeletal pyroxene crystals. In lithology B, non-vesicular impact melt occurs between the pyroxene and maskelynite grains and varies in composition between bulk B and maskelynite (figure 11). Solberg and Burns (1989) could not find evidence of Fe^{+3} in lithology C using Mössbauer spectroscopy. Based on their finding of high S in the glass veins, Rao *et al.* (1999) conclude that glass pods and veins in EETA79001 are a mixture of lithology A, excess plagioclase and Martian soil. However, Walton *et al.* (2010) did not find evidence for oxidized S in the glass pod they studied (Echo?).

SiO_2 : McSween and Jarosewich (1983) reported tridymite (?) associated with pyroxferroite (?) in the mesostasis of lithology B.

Whole-rock Composition

Ma *et al.* (1982), McSween and Jarosewich (1983), Burghelle *et al.* (1983), Smith *et al.* (1984), Treiman *et al.* (1994a) and Warren and Kallemeyn (1997) give complete analyses of both lithologies A and B in EETA79001 (tables 2 and 3). The Fe/Mg ratio and Al, K, REE and P contents of lithology B are significantly higher than for lithology A. Siderophiles have been determined by Kong *et al.* (1999), Warren *et al.* (1999), Neal *et al.* (2001), Putchel *et al.* (2008) and Walker *et al.* (2009). The Cr, Ni, Re, Os, Ir and Au contents are higher in lithology A than in B (see Warren *et al.*). The

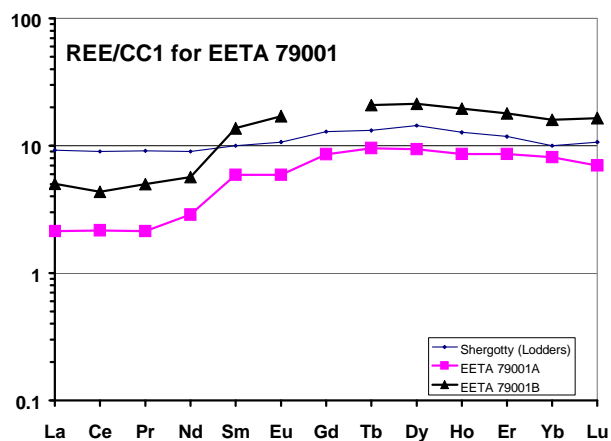


Figure 15. Normalized rare earth element diagram comparing the compositions of lithology A and B in EETA79001 with that of Shergotty.

REEs are compared with other Martian meteorites in figure 15.

Gibson *et al.* (1985) reported 2540 ppm S in lithology A and 1940 ppm S in lithology B. Jovanovic and Reed (1987) reported 9.4 ppb Hg. Dreibus *et al.* (1985) determined halogen contents, finding “mysterious excess I”. Multiple analyses of halogens would seem to be a way to determine if Martian soil was incorporated into the melt. The excess and irregular abundance of ^{36}Ar may be an indication of this.

Gooding *et al.* (1990) determined the thermal release pattern for several volatile species. Karlsson *et al.* (1992) determined 640 ppm H_2O in lithology A, but some of this may be adsorbed terrestrial water. Leshin *et al.* (1996) showed that most water in lithology A was released before 350°C.

Note that the data for major element compositions of A and B in the review paper by McSween (1985) are in the wrong columns in their paper!

Radiogenic Isotopes

Wooden *et al.* (1982), reported Rb/Sr isochrons 173 ± 10 m.y. with $I_{\text{Sr}} = 0.71217 \pm 3$ for lithology A and 185 ± 25 m.y. with $I_{\text{Sr}} = 0.71243 \pm 7$ for lithology B ($\lambda_{\text{Rb}} = 1.39 \times 10^{-11} \text{ year}^{-1}$). Nyquist *et al.* (2001) re-determined the Rb-Sr the age of lithology B as 174 ± 3 m.y. with $I_{\text{Sr}} = 0.712564 \pm 11$ (figure 16). *These apparent crystallization ages are apparently concordant with the shergottites and ALHA77005, but the range in initial Sr ratios indicates separate source rocks. However, please note that they have three or more*

Table 2a. Chemical composition of EETA79001 lithology A.

	McSween 83	Burghelle 83	Smith 84	Treiman 94a	Laul 86	Ma 82	Warren 97	Warren 97/Lee 98	
<i>weight</i>			<i>310 mg</i>	<i>67 mg *</i>	<i>310 mg</i>	<i>310 mg</i>	<i>312 mg</i>	<i>321 mg</i>	
SiO ₂ %	48.52 (a)	48.58 (b)					51.65	50.57	
TiO ₂	0.7 (a)	0.64 (b)	0.6 (d)		0.6 (d)	0.6 (d)	0.95	0.70	
Al ₂ O ₃	5.68 (a)	5.37 (b)	5.6 (d)		5.6 (d)	5.6 (d)	7.18	5.85	
Fe ₂ O ₃	0.7 (a)								
FeO	17.94 (a)	18.32 (b)	19.1 (d)	18.4 (d)	19 (d)	19.2 (d)	16.72	18.52	
MnO	0.52 (a)	0.469 (b)	0.47 (d)		0.47 (d)	0.469 (d)	0.47	0.49	
CaO	7.1 (a)	7.05 (b)	6.9 (d)	7 (d)	6.9 (d)	6.9 (d)	8.54	7.42	
MgO	16.59 (a)	16.31 (b)	16.3 (d)		16.3 (d)	16.3 (d)	11.9	14.6	
Na ₂ O	0.84 (a)	0.818 (b)	0.87 (d)	0.92 (d)	0.86 (d)	0.87 (d)	0.89	0.80	
K ₂ O	0.05 (a)	0.033 (b)	0.042 (d)		0.042 (d)	0.04 (d)	0.04	0.04	
P ₂ O ₃	0.65 (a)	0.54 (b)							
sum	99.29	98.13					98.34	98.99	
Li ppm		4.54 (b)							
C	200	36 (b)							
F		39 (b)							
S	1784 (g)	1600 (b)							
Cl		26 (b)							
Sc		36.1 (b)	37 (d)	37 (d)	36 (d)	37 (d)	37.2	38	
V			210 (d)		210 (d)	210 (d)	230	220	
Cr	3968 (a)	4030 (b)	4173 (d)	4392 (d)	4173 (d)	4173 (d)	4290	4760	
Co		47.3 (b)	48 (c)	48.9 (d)	45 (d)	48 (d)	43	55	
Ni	300	158 (b)	140 (d)	160 (d)		150 (d)	128	179	
Cu									
Zn		81 (b)	64 (c)		70 (d)		85	65	
Ga		12.6 (b)	13 (c)				14.2	12.8	
Ge									
As		0.005 (b)	0.044 (c)						
Se		<.8 (b)	0.43 (c)	0.5 (d)				<0.53	
Br		0.189 (e)							
Rb			1.04 (c)				<6.9	<4.3	
Sr		57 (b)	57				<46	<59	
Y									
Zr							67	44	
Nb									
Mo									
Pd ppb									
Ag ppb			19 (d)						
Cd ppb			37 (c)						
In ppb			46 (c)						
Sb ppb		<10 (b)	10 (c)						
Te ppb			5.9 (c)						
I ppm		<0.1 (b)							
Cs ppm			0.075 (c)	0.07 (d)			<0.103	<0.12	
Ba		<10 (b)					<26	<18	
La		0.37 (b)	0.41 (d)	0.32 (d)	0.41 (c)	0.42 (d)	0.48	0.41	
Ce		1.4 (b)	<0.5 (d)	1.4 (d)	1 (c)		1.71	1.13	
Pr									
Nd		1.4 (b)			1.3 (c)		<1.2	<2.6	
Sm		0.75 (b)	0.74 (d)	0.64 (d)	0.78 (c)	0.78 (d)	0.78	0.76	
Eu		0.35 (b)	0.37 (d)	0.331 (d)	0.37 (c)	0.38 (d)	0.40	0.37	
Gd									
Tb		0.3 (b)	0.26 (d)	0.25 (d)	0.34 (c)	0.24 (d)	0.32	0.32	
Dy		2.11 (b)	1.7 (d)			1.7 (d)	2.1	2.2	
Ho		0.5 (b)			0.5 (c)		0.4	0.49	
Er									
Tm		0.21 (b)	0.11 (d)		0.22 (c)				
Yb		1.12 (b)	1.1 (d)	1.03 (d)	1.25 (c)	1.11 (d)	1.16	1.11	
Lu		0.15 (b)	0.18 (d)	0.14 (d)	0.18 (c)	0.19 (d)	0.17	0.16	
Hf		0.93 (b)	0.94 (d)	0.97 (d)	0.94 (c)	0.97 (d)	0.97	0.98	0.8198 (f)
Ta		0.03 (b)	<0.05 (d)	0.03 (d)			<0.08	0.03	
W ppb		83 (b)							0.07709 (f)
Re ppb									
Os ppb									
Ir ppb		<2 (b)					<2.3	<5	
Au ppb		2.8 (b)	3.9 (c)	18 (d)			<2	0.96	
Tl ppb			6.9 (c)						
Bi ppb	Chen 86		0.67 (c)						
Th ppm	0.08 (f)	<.1 (b)					<0.1	<0.07	
U ppm	0.018 (f)	<.06 (b)					<0.16	<0.04	

technique (a) wet chem., (b) INAA & RNAA, (c) RNAA, (d) INAA, (e) Dreibus et al 1985, (f) isotope dilution mass spec. (g) recalculated

* from powder prepared by Jarosewich

Table 2b. Chemical composition of EETA79001 lithology A (cont.).

reference weight	Lodders 98 average	Kong 99 100.7 mg.	Mittlefehldt 99 543 mg.	Warren 99 290 mg.	Warren 99 297 mg.	Neal 2001	Neal 2001		
SiO ₂	49.9			51.56	50.49				
TiO ₂	0.7	1.67	(a)	0.95	0.7	(a)		0.69	
Al ₂ O ₃	5.91	7.71	(a)	7.18	5.86	(a)		6.12	
FeO	18.4	20.07	(a)	16.72	18.53	(a)		24.3	
MnO	0.48	0.53	(a)	0.47	0.49	(a)		0.54	
CaO	7.26	8.02	(a) 7.7	(a) 8.5	7.4	(a)		7.86	
MgO	16.1	17.58	(a)	11.94	14.59	(a)		16.9	
Na ₂ O	0.86	0.77	(a) 0.87	(a) 0.89	0.795	(a)		1.06	
K ₂ O	0.04	0.035	(a) 0.05	(a) 0.04	0.04	(a)			
P ₂ O ₅	0.6							0.66	
sum									
Li ppm	4.5							1.47	1.69 (d)
Sc	36	36.7	(a) 45.3	(a) 37.2	38	(a)		30.2	32.2 (d)
V	210	234	(a)	230	220	(a)		195.5	189.4 (d)
Cr	4240	4230	(a) 2830	(a) 4290	4760	(a)		3533	3733 (d)
Co	48	59.4	(a) 42.2	(a) 43	55	(a)		44.6	46.4 (d)
Ni	180			123	166	(b)		139.4	147.4 (d)
Cu								11.7	11.7 (d)
Zn	73	87.2	(a)	72	66	(b)		67.7	70.1 (d)
Ga	13.2	13.4	(a)	14.2	12.8	(a)		12.1	12.8 (d)
Ge				0.87	0.8	(b)			
As	0.005		0.22	(a) <0.4		(a)			
Se	0.47				<0.53	(a)			
Br	0.141			0.32	0.28	(a)			
Rb	1.04		2	(a)				1.24	1.27 (d)
Sr	57		20	(a) <46	<59	(a)		20.7	18.3 (d)
Y								10.7	12.4 (d)
Zr	29.4		60	(a) <100	<90	(a)		28.5	29.7 (d)
Nb	0.68							0.8	0.86 (d)
Mo		0.01	(b)					0.19	0.26 (d)
Pd ppb						6.05	(d)		
Ag ppb	19	5.3	(b)						
Cd ppb	37			12.3		(b)			
In ppb	46								
Sb ppb	10		15	(a)				20	10 (d)
Te ppb	5.9								
I ppm	<0.1								
Cs ppm	0.073			<0.103	<0.12	(a)		0.06	0.07 (d)
Ba	<10		12	(a)				4.99	5.56 (d)
La	0.4	0.46	(a) 0.43	(a) 0.48	0.41	(a)		0.5	0.5 (d)
Ce	1.27	0.87	(a) 1.5	(a) 1.71	1.13	(a)		1.26	1.3 (d)
Pr								0.19	0.19 (d)
Nd	1.35			<1.2	<2.6	(a)		1.03	1.3 (d)
Sm	0.74	0.833	(a) 0.78	(a) 0.78	0.76	(a)		0.74	0.87 (d)
Eu	0.37	0.405	(a) 0.36	(a) 0.4	0.37	(a)		0.38	0.33 (d)
Gd		0.59	(a)					1.53	1.69 (d)
Tb	0.28	0.347	(a) 0.32	(a) 0.32	0.32	(a)		0.33	0.35 (d)
Dy	1.9			2.1	2.2	(a)		2.15	2.28 (d)
Ho	0.5			0.4	0.49	(a)		0.45	0.48 (d)
Er								1.32	1.37 (d)
Tm	0.18							0.18	0.19 (d)
Yb	1.12	1.32	(a) 1.28	(a) 1.16	1.11	(a)	Blichert-Toft 99	1.24	1.32 (d)
Lu	0.17	0.172	(a) 0.18	(a) 0.17	0.16	(a)	0.156 (c)	0.17	0.17 (d)
Hf	0.95	1.01	(a) 1.09	(a) 0.97	0.98	(a)	0.936 (c)	0.84	1.03 (d)
Ta	0.03		0.08	(a) <0.08	0.03	(a)		0.05	0.05 (d)
W ppb	83	33	(b) 200	(a)			Brandon 2000	70	90 (d)
Re ppb				0.23	0.085	(b)	0.0989 (c)		
Os ppb		1.5	(b)	2.3	1.55	(b)	0.4811 (c)		
Ir ppb		1.64	(b)	2	1.42	(b)	0.59 (d)		
Au ppb	2.6	0.803	(b) 3.2	(a) 0.92	0.8	(b)			
Pt ppb	0.67	6.38	(b)				8.65 (d)		
Ru ppb		2.2	(b)				1.6 (d)		
Rh ppb							0.88 (d)		
Tl ppb	6.9								
Th ppm	0.08		0.07	(a) <0.1	<0.07	(a)		0.15	0.15 (d)
U ppm	0.019			<0.16	<0.04	(a)		0.02	0.02 (d)

technique (a) INAA, (b) RNAA, (c) IDMS, (d) ICP-MS

Table 3a. Chemical composition of EETA79001 lithology B.

	McSween 83	Burghelle 83	Smith 84	Treiman 94a	Laul 86	Dreibus 96	Ma 82	Warren 97	Warren 97
<i>weight</i>		232.7	301 mg	71 mg *	301 mg		301 mg	319 mg	324 mg
SiO ₂ %	49.03 (a)	49.03 (b)						49.72	49.93
TiO ₂	1.23 (a)	1.12 (b)	1.1 (d)		1.1 (d)		1.1 (d)	1.53	1.25
Al ₂ O ₃	9.93 (a)	9.93 (b)	10.5 (d)		10.5 (d)		10.5 (d)	11.7	13.4
Fe ₂ O ₃	0.22 (a)								
FeO	16.87 (a)	17.74 (b)	17.9 (d)	17.3 (d)	17.9 (d)		17.9 (d)	17.62	16.97
MnO	0.47 (a)	0.452 (b)	0.41 (d)		0.41 (d)		0.413 (d)	0.41	0.41
CaO	11 (a)	10.99 (b)	10.4 (d)	11.3 (d)	10.4 (d)		10.4 (d)	10.92	10.78
MgO	7.32 (a)	7.38 (b)	7.5 (d)		7.5 (d)		7.5 (d)	5.47	5.14
Na ₂ O	1.68 (a)	1.66 (b)	1.62 (d)	1.69 (d)	1.62 (d)		1.62 (d)	1.78	2.03
K ₂ O	0.09 (a)	0.065 (b)	0.075 (d)		0.075 (d)		0.07 (d)	0.08	0.08
P ₂ O ₃	1.25 (a)	1.31 (b)							
sum	99.09	99.677						99.23	99.99
Li ppm		2.21 (b)							
C	100	98 (b)							
F		30.9 (b)							
S	2184 (f)	1920 (b)							
Cl		48 (b)							
Sc		50.5 (b)	50 (d)	50.1 (d)	50 (d)		50 (d)	43.2	42.1
V			206 (d)		206 (d)		206 (d)	159	135
Cr	957 (a)	1252 (b)		1273 (d)	1197			650	420
Co	<100	31.1 (b)	30 (c)	30.8 (d)	30 (d)		30 (d)	27.7	28.4
Ni	<100	46 (b)	30 (d)	50 (d)			20 (d)	23	19
Cu									
Zn		120 (b)	71 (c)		71 (d)			105	92
Ga		24.4 (b)	17 (c)					26.8	29.9
Ge									
As		0.012 (b)	0.021 (c)						
Se			0.42 (c)	0.4 (d)					1.83
Br		0.289 (e)							
Rb			1.78 (c)					<6.9	<4.1
Sr		67 (b)	67	40 (d)				34	28
Y						27.8 (g)			
Zr						64.8 (g)		64	90
Nb						1.66 (g)			
Mo									
Pd ppb									
Ag ppb			6.3 (c)						
Cd ppb			70 (c)						
In ppb			68 (c)						
Sb ppb		<30 (b)	16 (c)						
Te ppb			7.4 (c)						
I ppm		0.96 (b)							
Cs ppm			0.131 (c)	0.13 (d)				0.159	<0.13
Ba		14 (b)				12 (g)		<50	<26
La		0.8 (b)	0.81	0.68 (d)	0.88 (c)	0.781 (g)	0.82 (d)	1.18	1.03
Ce		3.1 (b)	2.2	1.6 (d)	2.2 (c)	2 (g)		2.63	2.34
Pr									
Nd		2.9 (b)	3		2.5 (c)	2.12 (g)	3 (d)	2.55	3.1
Sm		1.56 (b)	1.5	1.28 (d)	1.65 (c)	1.43 (g)	1.5 (d)	2.01	1.95
Eu		0.73 (b)	0.72		0.72 (c)	0.67 (g)	0.72 (d)	0.96	0.95
Gd					3.2 (c)	2 (g)			
Tb		0.64 (b)	0.57	0.64 (d)	0.71 (c)	0.48 (g)	0.55 (d)	0.76	0.79
Dy		4.58 (b)	3.7			3 (g)	3.7 (d)	5.2	5.1
Ho		0.99 (b)			0.98 (c)	0.71 (g)		1.09	1.08
Er									
Tm		0.37 (b)	0.27		0.4 (c)				
Yb		2.14 (b)	2	1.81 (d)	2.3 (c)	1.85 (g)	2.04 (d)	2.61	2.65
Lu		0.3 (b)	0.3	0.25 (d)	0.32 (c)	0.26 (g)	0.3 (d)	0.4	0.38
Hf		1.93 (b)	1.77	1.78 (d)	1.77	1.84 (g)	1.81 (d)	2.26	2.31
Ta		0.09 (b)	0.09	0.06 (d)				0.09	0.068
W ppb		155 (b)							
Re ppb									
Os ppb									
Ir ppb		<3 (b)						<1.3	<2.4
Au ppb		1.1 (b)	0.82 (c)					<1.0	<0.2
Tl ppb			7.9 (c)						
Bi ppb			0.76 (c)						
Th ppm		<0.2 (b)				0.144 (g)		0.14	0.15
U ppm		<0.1 (b)		0.11 (d)		0.0366(g)		<0.24	<0.07

technique (a) wet chem., (b) INAA & RNAA, (c) RNAA, (d) INAA, (e) Dreibus et al 1985, (f) recalculated, (g) spark source mass spec *from powder prepared by Jarosewich

Table 3b. Chemical composition of EETA79001 lithology B (cont.)

reference weight	Lodders 98 average	Blichert-Toft 99				Warren 99		Brandon 2000	
		275 mg	259 mg	233 mg	92 mg.	297 mg	305 mg.	202 mg.	
SiO ₂	49.4					49.63	49.85		
TiO ₂	1.18					1.53	1.25	(a)	
Al ₂ O ₃	11.2					11.71	13.41	(a)	
FeO	17.4					17.62	16.98	(a)	
MnO	0.43					0.41	0.41	(a)	
CaO	10.8					10.91	10.78	(a)	
MgO	6.57					5.47	5.14	(a)	
Na ₂ O	1.74					1.78	2.03	(a)	
K ₂ O	0.075					0.08	0.08	(a)	
P ₂ O ₅	1.28								
sum	100.075								
Li ppm	2.2								
Sc	47					43.2	42.1	(a)	
V	190					159	135	(a)	
Cr	1150					650	420	(a)	
Co	29					27.7	28.4	(a)	
Ni	28					17	14.3	(b)	
Cu									
Zn	91					89	87	(b)	
Ga	21					26.8	29.9	(a)	
Ge						0.69	0.88	(b)	
As	0.017					<0.7			
Se	0.41						<2	(a)	
Br	0.025					0.5	0.4	(a)	
Rb	1.78								
Sr	54					34	28	(a)	
Y	28								
Zr	64.8					64	90	(a)	
Nb	1.66								
Mo									
Pd ppb									
Ag ppb	6.3								
Cd ppb	70								
In ppb	68								
Sb ppb	16								
Te ppb	7.4								
I ppm	0.96								
Cs ppm	0.13					159	<130	(a)	
Ba	13								
La	0.85					1.18	1.03	(a)	
Ce	2.13					2.63	2.34	(a)	
Pr									
Nd	2.63					2.55	3.1	(a)	
Sm	1.66					2.01	1.95	(a)	
Eu	0.78					0.96	0.95	(a)	
Gd	2.7								
Tb	0.62					0.76	0.76	(a)	
Dy	3.76					5.2	5.1	(a)	
Ho	0.89					1.09	1.08	(a)	
Er									
Tm	0.35								
Yb	2.02					2.61	2.65	(a)	
Lu	0.31	0.262	0.302	0.315	0.211	(c)	0.4	0.38	(a)
Hf	1.87	2.01	2.1	2.29	1.47	(c)	2.26	2.31	(a)
Ta	0.08						0.087	0.068	(a)
W ppb	140								
Re ppb						0.0109	0.0166	(b)	0.0658 (c)
Os ppb						0.0029	0.0055	(b)	0.1597 (c)
Ir ppb	<3					0.00189	0.00061	(b)	
Au ppb	0.96					0.25	0.8	(b)	
Pt ppb	0.76								
Ru ppb									
Tl ppb	7.9								
Bi ppb	0.76								
Th ppm	0.145					0.14	0.15	(a)	
U ppm	0.037					<0.24	<0.07	(a)	

technique (a) INAA, (b) RNAA, (c) IDMS

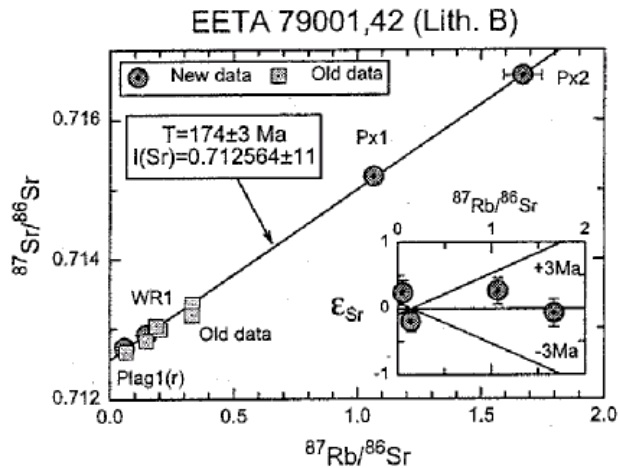


Figure 16. Rb-Sr internal mineral isochron for EETA79001B. This is figure 1 in Nyquist *et al.* XXXII.

“cosmic ray exposure ages” (see below).

Nyquist *et al.* (1984) also reported a Sm-Nd isochron age for pyroxene - whole rock as 240 ± 150 m.y., but made no further reference to this age in Nyquist *et al.* (1986). Wooden *et al.* (1982) determined the Sm-Nd model age of 2.6 b.y. Nyquist *et al.* (2001) determined a precise Sm-Nd internal isochron for lithology B with an age of 169 ± 23 m.y. and initial $\epsilon_{Nd} = +16.6 \pm 1.4$ (figure 17).

Nyquist *et al.* (1984) analyzed hand-picked “mafic xenocrysts” from lithology A and found that they had $I_{Sr} = 0.71187 \pm 7$ (calculated for 180 m.y.). However, Nyquist later revised this number to be on the isochron (personal communication). Nyquist *et al.* (1986) analyzed the I_{Sr} in glass inclusions (lithology C) and found that they were heterogeneous (figure 18).

By leaching “whole-rock” samples of EETA79001, Chen and Wasserburg (1986a) obtained a U-Pb

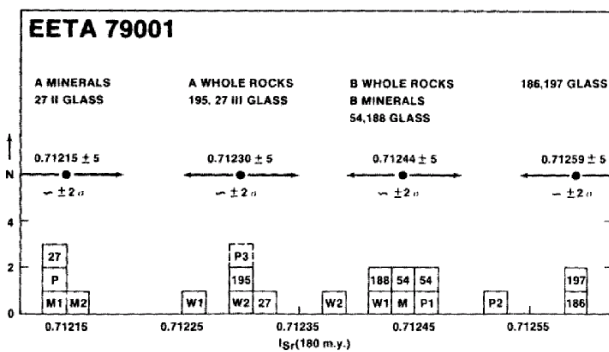


Figure 18. Initial Sr isotopic composition of glass “pods” in EETA79001. This is figure 4 in Nyquist *et al.* 1986, LPS XVI.

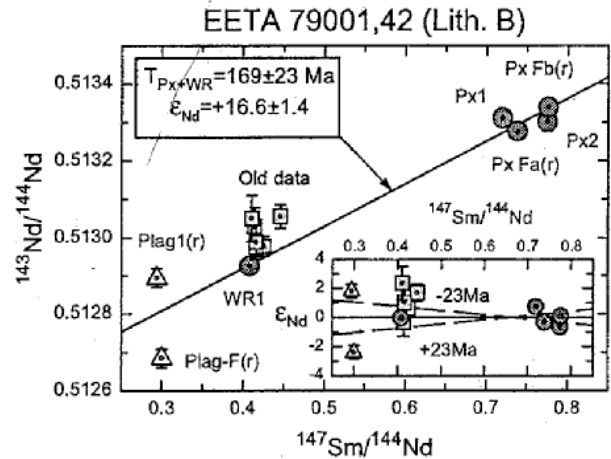


Figure 17. Sm-Nd internal mineral isochron for EETA79001B. This is figure 2 in Nyquist *et al.* XXXII.

“isochron” of 150 ± 15 m.y. and a Th-Pb “isochron” of 170 ± 36 m.y. These leach experiments probably attacked the phosphates in the sample.

It has not proven possible to date the crystallization age of EETA79001 by Ar39-40 technique (see Bogard and Garrison 1999).

Compiler’s Note: This rock has multiple features that require dating. First, there was an event that made the source region for the materials in this rock. Then, there were two igneous events when lithologies

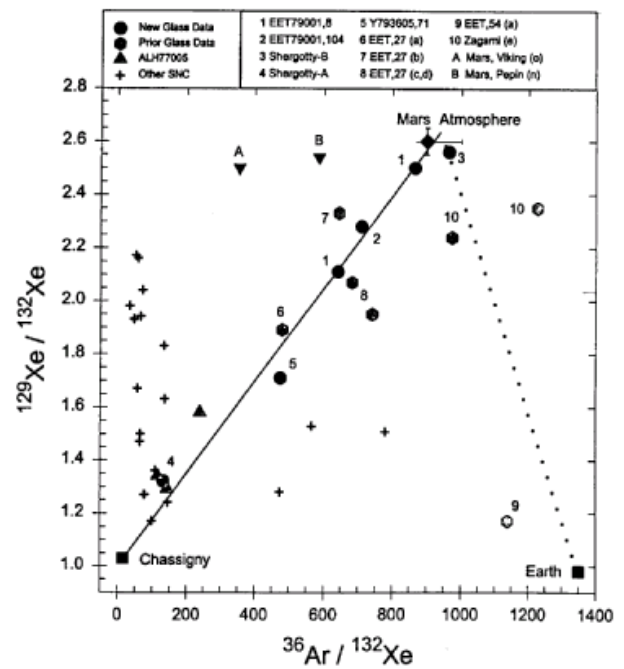


Figure 19. Rare gas composition of Martian meteorites compared with Viking mission. This figure is from Bogard and Garrison 1999.

Isotopic Results on “White-Druse”

	$\delta^{13}\text{C}$	$\delta^{18}\text{O}$	^{14}C	$\delta^{15}\text{N}$
Clayton and Mayeda (1988)	+9.7 ‰	+21.0 ‰		
Wright <i>et al.</i> (1988)	+6.8 ‰	+21.0 ‰		~0 ‰
Jull <i>et al.</i> (1992)	+3.1 ‰	+20.0 ‰	<i>high activity</i>	
Douglas <i>et al.</i> (1994)	+7.2 and -28.6 ‰			

A and B crystallized. Later, there was a shock event that converted the plagioclase into maskelynite and perhaps another shock event that formed the glass pods and veins and also trapping the Martian atmosphere. There may have been a time when the rock was altered by fluids on Mars (forming the salts observed in the void) and there was an event that launched this rock from Mars. Finally, there was a length of time during which the rock was in Antarctica. Which age goes with which event?

Cosmogenic Isotopes and Exposure Ages

Jull and Donahue (1988) give a terrestrial exposure age of 12 ± 2 thousand years using ^{14}C . However, Sarafin *et al.* (1985) reported a “terrestrial residence time” of 320 ± 170 thousand years. Nishiizumi *et al.* (1986) set a limit of <60 thousand years using ^{36}Cl on a deep sample (2.5 cm) and the terrestrial age for this sample remains poorly determined.

Bogard *et al.* (1984b) determined a cosmic-ray exposure age of ~0.5 m.y. Sarafin *et al.* (1985) reported an exposure age of 0.78 ± 0.14 m.y. Nishiizumi *et al.* (1986) reported an exposure age of 0.6 m.y. Pal *et al.* (1986) determined exposure ages of 0.73 ± 0.19 m.y. for lithology A and 0.9 ± 0.17 m.y. for lithology B using ^{10}Be . Schnabel *et al.* (2001) determined 0.70 ± 0.06 using ^{10}Be . Nyquist *et al.* (2001) give a “preferred exposure age” of 0.6 ± 0.09 m.y. (*much younger than for the other Martian meteorites*).

Hidaka *et al.* (2001) have determined the isotopic ratios of Sm and Gd, both sensitive to thermalized neutrons caused by cosmic ray interaction with the Martian surface. Excess ^{36}Ar and ^{80}Kr may also be due to neutron irradiation of Cl- and Br-rich Martian soil that has been incorporated into lithology A (Rao *et al.* 1999).

Other Isotopes

This is the rock that demonstrated the Martian origin for SNC meteorites (*see* Pepin 1985; Hunten *et al.* 1987; or review by McSween 1985, 1994). In glass pockets of this meteorite, Bogard and Johnson (1983)

and Bogard *et al.* (1984b) found high concentrations of rare gasses and determined that the ratios $^{84}\text{Kr}/^{132}\text{Xe}$ ~15, $^{40}\text{Ar}/^{36}\text{Ar} > 2000$, $^{129}\text{Xe}/^{132}\text{Xe} > 2$ and $^4\text{He}/^{40}\text{Ar} < 0.1$ were significantly different than the rare gas component of any other meteorite, but indeed similar to the rare gas analysis made by the Viking spacecraft on Mars. Becker and Pepin (1984) extended this observation to $^{15}\text{N}/^{14}\text{N}$ and N/Ar ratios. Ott and Begemann (1985), Wiens (1988) and others have extended and confirmed these measurements (*see also Marti *et al.* 1995 for similar data on Zagami*). Bogard and Garrison (1999) and Garrison and Bogard (1998) have made further detailed analyses and have developed improved correction procedures for adsorbed terrestrial gases and spallation components (table 5). With these improvements, they have now accurately determined the rare gas composition of the Martian atmosphere (*much more accurately than the Viking mass spectrometer could*) (figure 19).

Mathew *et al.* (1998) have studied both N and Xe isotopes by stepwise heating and distinguished three different gas components in EETA79001.

Clayton and Mayeda (1983, 1996) reported the oxygen isotopes for EETA79001 A and B. Romanek *et al.* (1996, 1998) and Franchi *et al.* (1999) reported additional data for oxygen isotopes using laser-fluoridation techniques.

Carr *et al.* (1985) calculated a heavy ^{13}C component ($\delta^{13}\text{C} = +36$ ‰) for the gas found in the high temperature release of lithology C in EETA79001 which may be from the atmosphere on Mars. However, this was based on very small amounts of carbon.

Clayton and Mayeda (1988) and Wright *et al.* (1988) determined $\delta^{13}\text{C}$ and $\delta^{18}\text{O}$ for “calcite” dissolved by phosphoric acid in “white druse” material supplied by Gooding (*see* figure 12, sample ,239). These authors concluded the “druse” was a product of extra-terrestrial origin (*i.e.* alteration on Mars). Jull *et al.* (1992) studied a different sample of “druse” (,320) and found that it

contained significant ^{14}C , which requires a terrestrial origin.

Wright *et al.* (1988) and Grady *et al.* (1995a) found that the nitrogen released from EETA79001 or its “druse” (carbonates) was not enriched in $\delta^{15}\text{N}$ and the apparent nitrates in these salts could not have formed by oxidation of the Martian atmosphere. Since the nitrates, carbonates and sulfates are all part of the same mineral assemblage, this also apparently creates a problem for a Martian origin of these salts.

Farquhar *et al.* (2000) and Franz *et al.* (2008) have reported S isotope analyses of multiple mineral phases. They are looking for evidence of a contribution of anomalous ^{33}S from the Mars atmosphere.

Leshin *et al.* (1996) extracted the water out of EETA79001 and measured the isotopic ratio of hydrogen at several temperature steps.

Chen and Wasserburg (1986) reported the Pb isotopes in EETA79001 and concluded that the parent body (Mars) was enriched in ^{204}Pb and (probably) other volatiles. Lead isotope studies of shergottites may prove definitive for the soil entrapment hypothesis (figure 38).

Lee and Halliday (1997) reported excess ^{182}W and Harper *et al.* (1995) reported a small ^{142}Nd anomaly indicating early differentiation of Mars (and lack of subsequent mixing). Lu-Hf and Re-Os systematics also support earlier arguments that chemical compositional variability resulting from this early differentiation has been preserved (Blichert-Toft *et al.* 1999; Brandon *et al.* 2000).

Schnabel *et al.* (2001) have determined the ^{26}Al , ^{10}Be and ^{53}Mn activity.

Organics (?)

Wright *et al.* (1989) and Gooding *et al.* (1990) reported organic compounds released during heating. Gooding *et al.* recognized that the trace organic concentration in their sample was not above background as determined on blanks (Gooding 1992). However, the low temperature release sample studied by Wright *et al.* (EETA79001,239) was reported to have ~ 1,000 ppm C with an isotopically light signature ($\delta^{13}\text{C} = -30\text{‰}$). Douglas *et al.* (1994) confirmed this result in a second sample (EETA79001,323) and stated “if the

carbonaceous components in 239 and 323 are truly martian organics, the implications for our understanding of Mars are immense.”

McDonald and Bada (1995) analyzed samples of “white druse” and lithology A from EETA79001 for amino acids and found approximately 1 ppm and 0.4 ppm respectively. However the amino acids detected were almost exclusively L-enantiomers commonly found in proteins and thus terrestrial contamination. They also found that the amino acids in clean Antarctic ice were of the same kind and concluded that the “white druse” could have been contaminated by organics from melt water in Antarctica. Becker *et al.* (1997) also reported on PAHs in EETA79001, ALH84001 and ice water (figure 20).

The possibility of organic contamination by Xylan (used as a lubricant in the processing cabinets) was examined and ruled out by Wright *et al.* (1992g). The possibility of bacterial action was first pointed out by Ivanov *et al.* (1992).

Shock Effects

Stöffler *et al.* (1986, 2000) determined that EETA79001 reached a shock pressure of 34 ± 1 GPa with post-shock temperature about 250°C . McSween and Jarosewich (1983) pointed out that bulk melting of

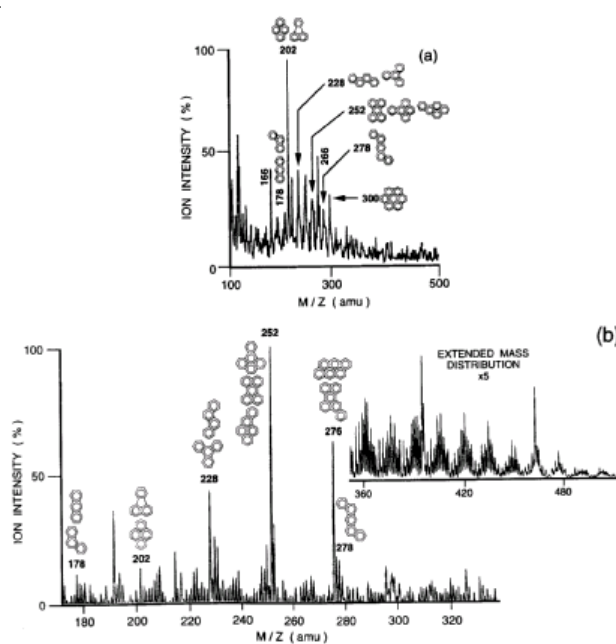


Figure 20. Mass spectra of organics released from (A) lithology A and (B) carbonate “druse” in EETA79001. This is figure 1 in Becker *et al.* 1997, GCA 61, 477.

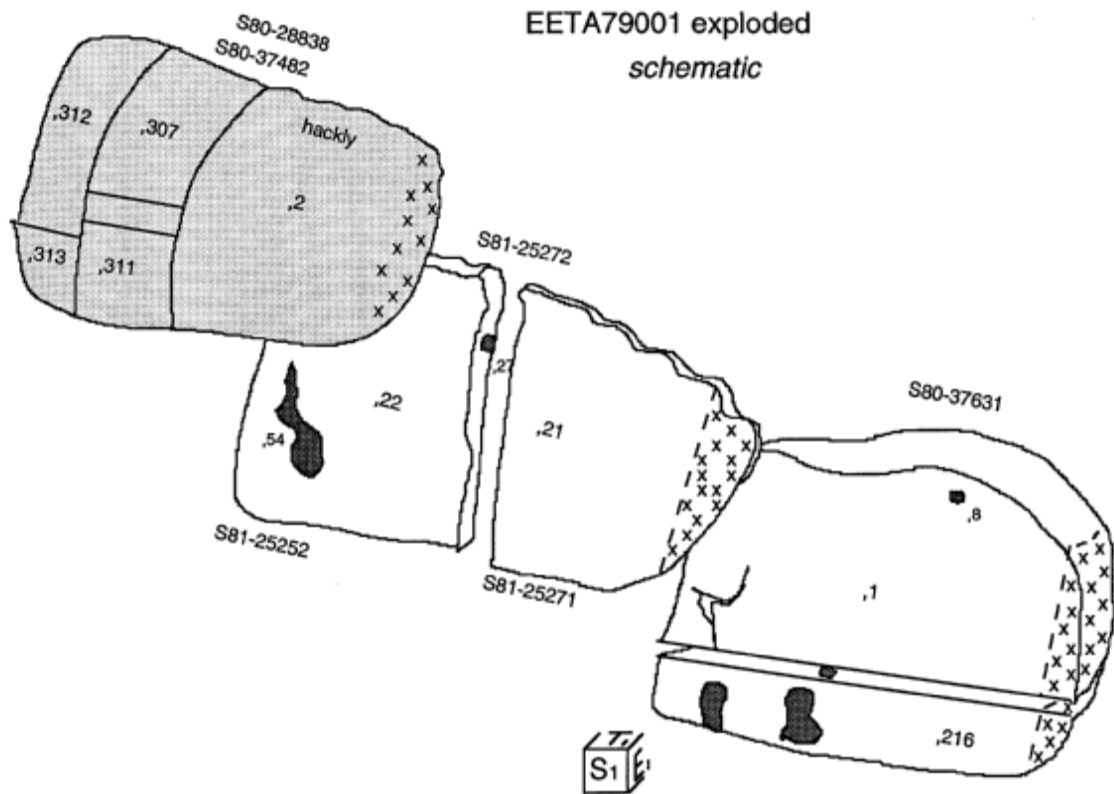


Figure 21. Exploded parts diagram for EETA79001.

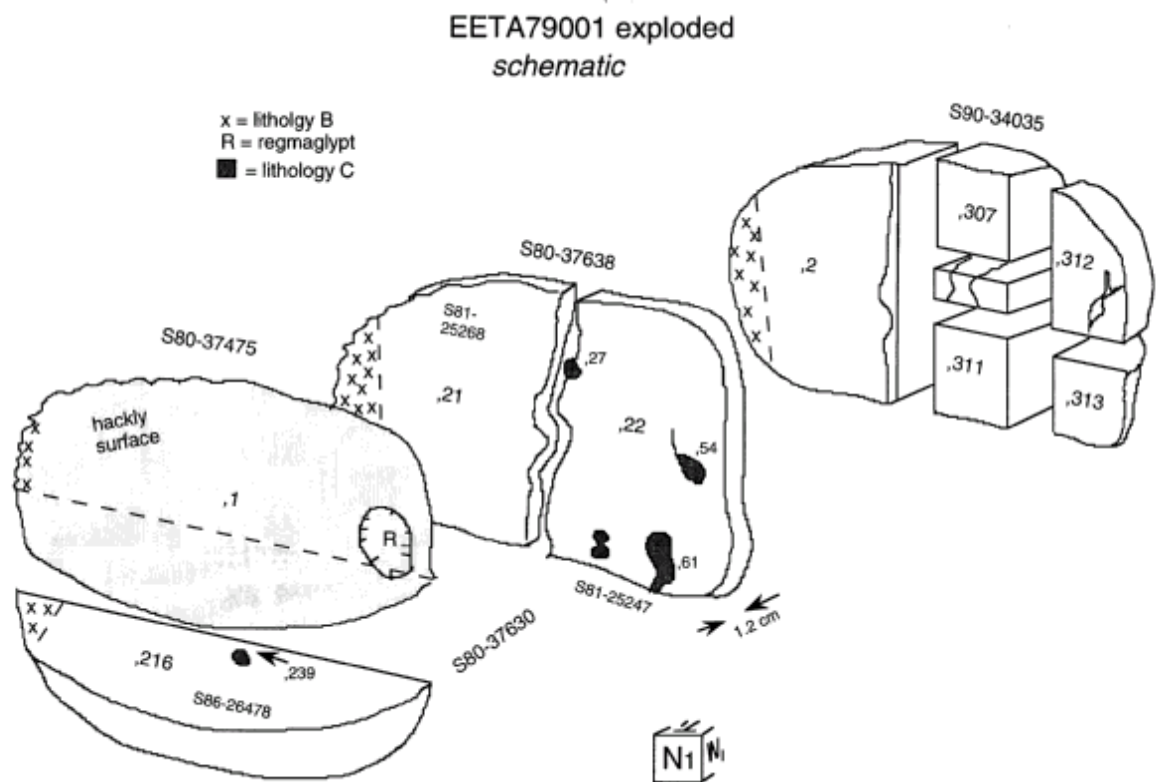


Figure 22. Exploded parts diagram for EETA79001 (reversed).

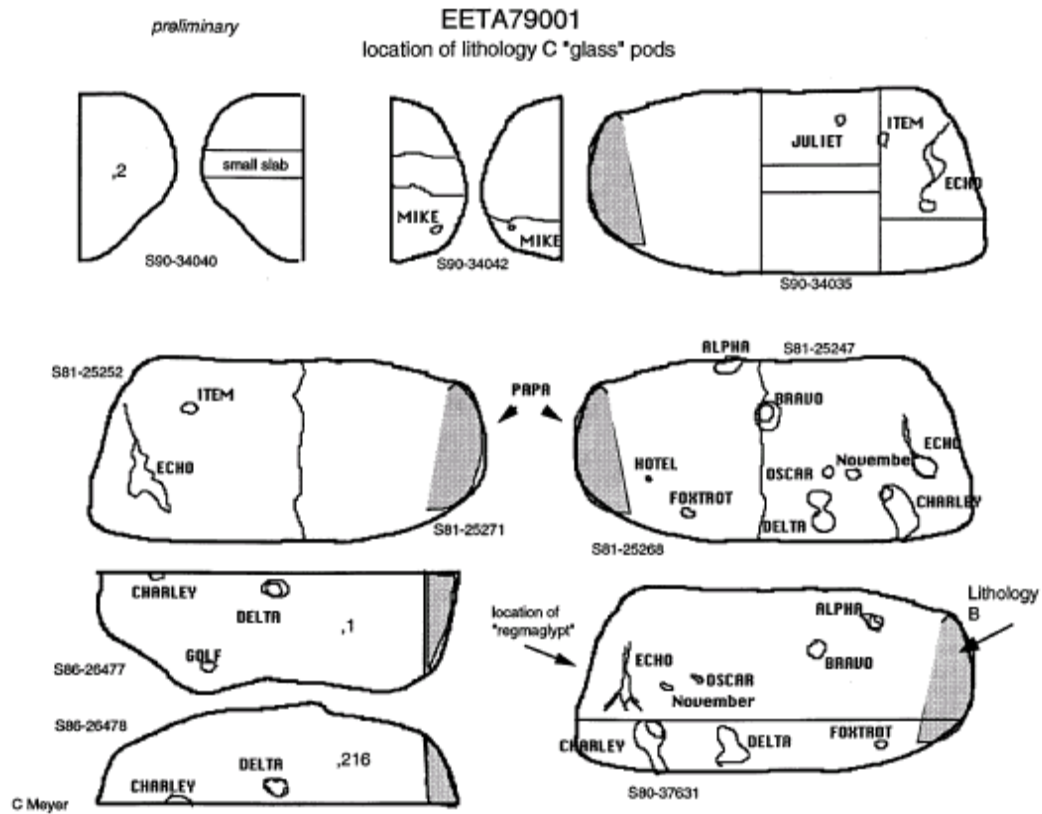


Figure 23. Location of glass "pods" on sawn surfaces of EETA79001 (see table IX-1). This sketch also illustrates the approximate location of lithology B (shaded).

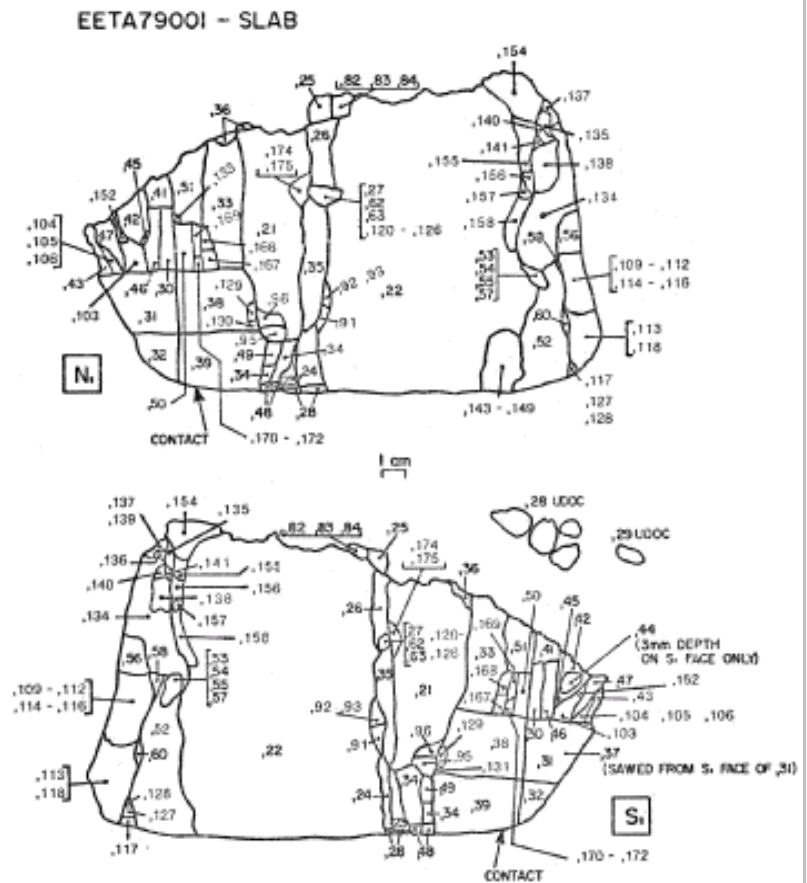


Figure 24. Allocation plan for slab ,22 used by McSween consortium.

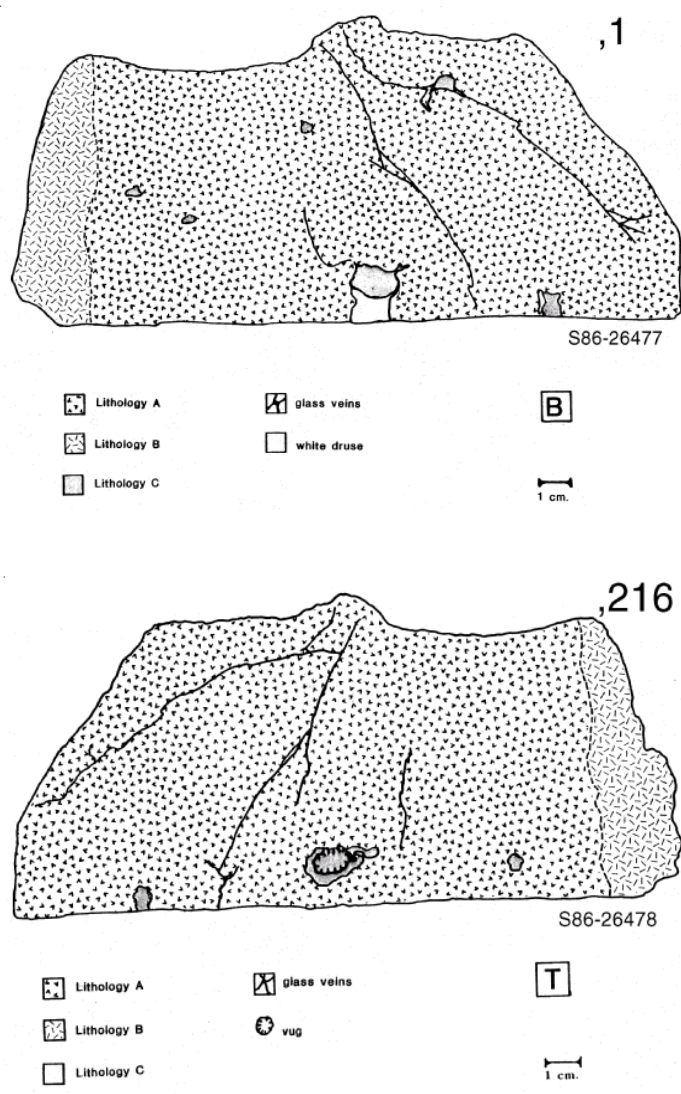


Figure 25. Lithological maps of sawn surfaces of EETA79001,1 and EETA79001,216. Drawings by R. Martinez and J. Gooding 1986.

lithology A, as indicated by the composition of the glass pods and veins, indicates shock pressures in excess of 80 GPa (Schaal and Hörz 1977). Boctor *et al.* (1998a,b) have reported evidence of high pressure phase transition and vitrification in olivine megacrysts from lithology A. Boctor *et al.* also reported the presence of majorite (?) in veins of shock glass in lithology B. However, the shock event that blasted this rock off Mars was apparently not intense enough to cause decrepidation of the carbonate salts (Gooding *et al.* 1988).

Other Studies

Wasylenki *et al.* (1993) performed melting experiments on the composition of the groundmass of lithology A, EETA79001. Longhi and Pan (1989) have

also performed experimental work related to the origin of shergottites.

EETA79001 possesses a “weak, very stable primary natural remanent magnetization (NRM)” (see table 3). Titanomagnetite, and possibly pyrrhotite, have been identified as the mineral phases that carry the magnetism (Cisowski 1982, 1985, 1986; Collinson 1986, 1997; and Terho *et al.* 1993). Collinson (1997) has estimated that the strength of the magnetizing field on Mars was in the range of 0.5-5 microTesla, which is at least an order of magnitude greater than the present field. Terho *et al.* (1998) has reported additional information on the magnetic properties of a piece of EETA79001.



Figure 26. Sawn face of EETA79001,1 after first saw cut (NASA # S80-37631). See figures 21 and 23. Sawing was done dry, with a steel band saw.

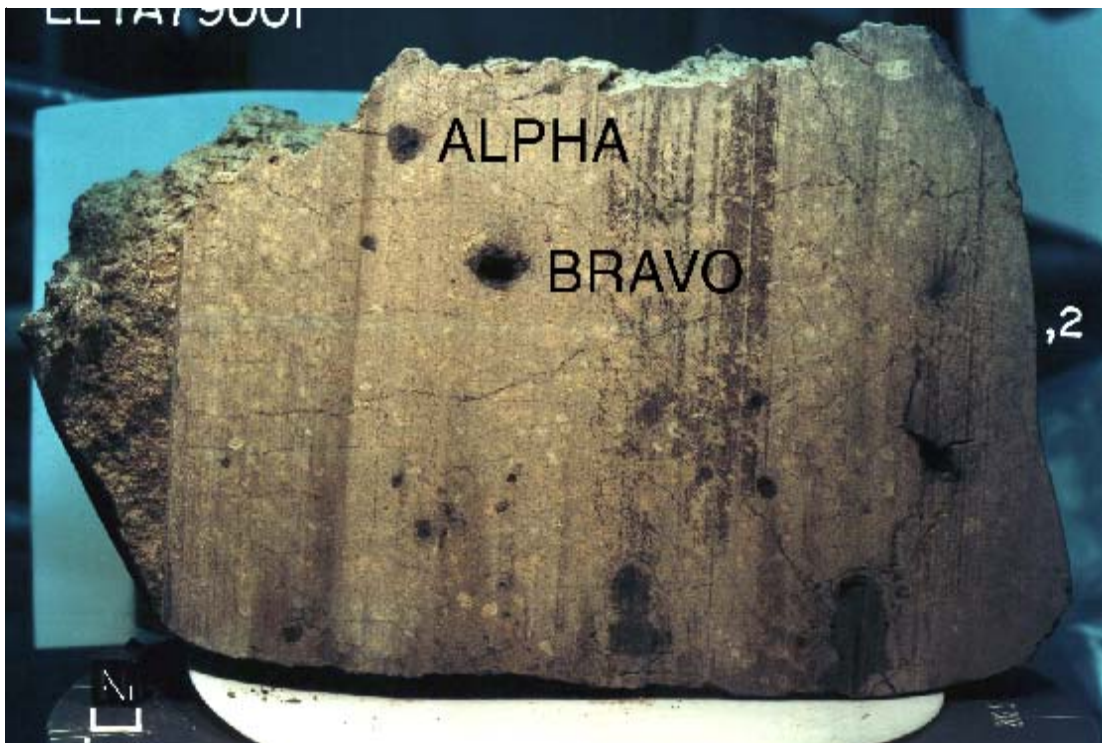


Figure 27. Sawn face of EETA79001,2 after first saw cut (NASA # S80-37632). This photo is prior to second saw cut. BRAVO is the glass inclusion (,27) where the discovery of Martian atmospheric gasses was made. Note the large vesicles in the glass pods.

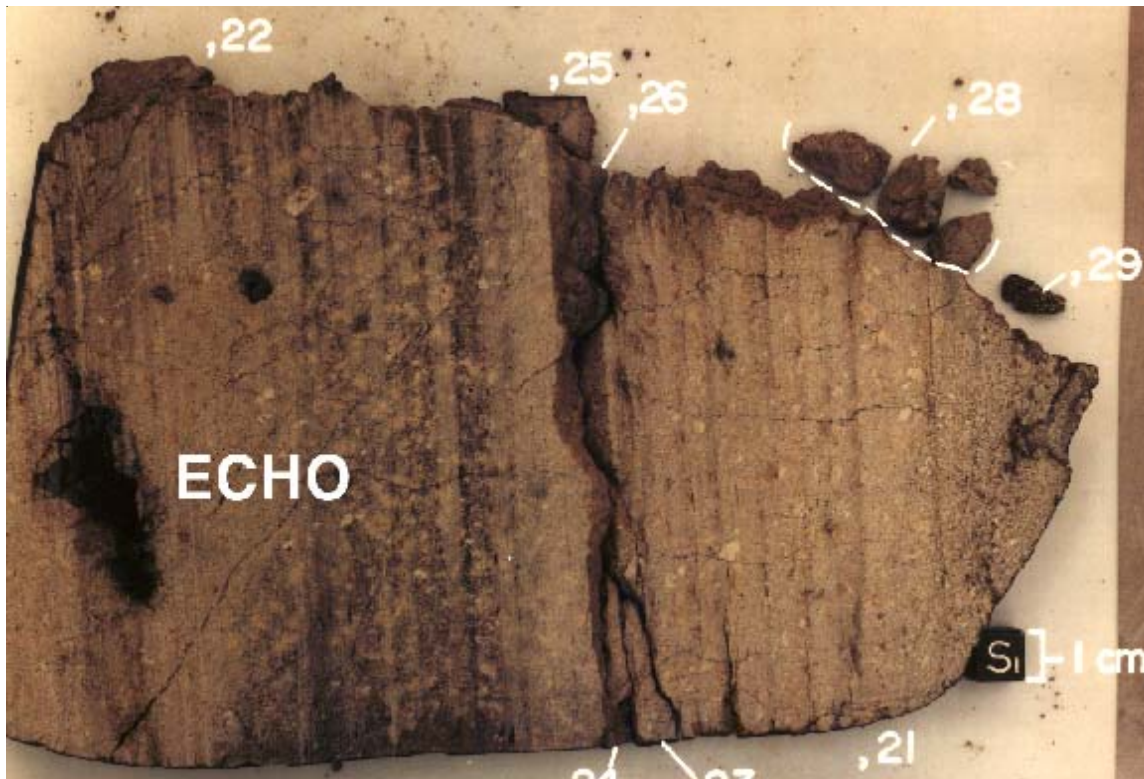


Figure 28. Photograph of complete slab through center of EETA79001 (see figure 21). Slab broke into two pieces ,21 and ,22. Note the basaltic texture of lithology B on the right end of ,21. This is NASA photo # S80-25272.

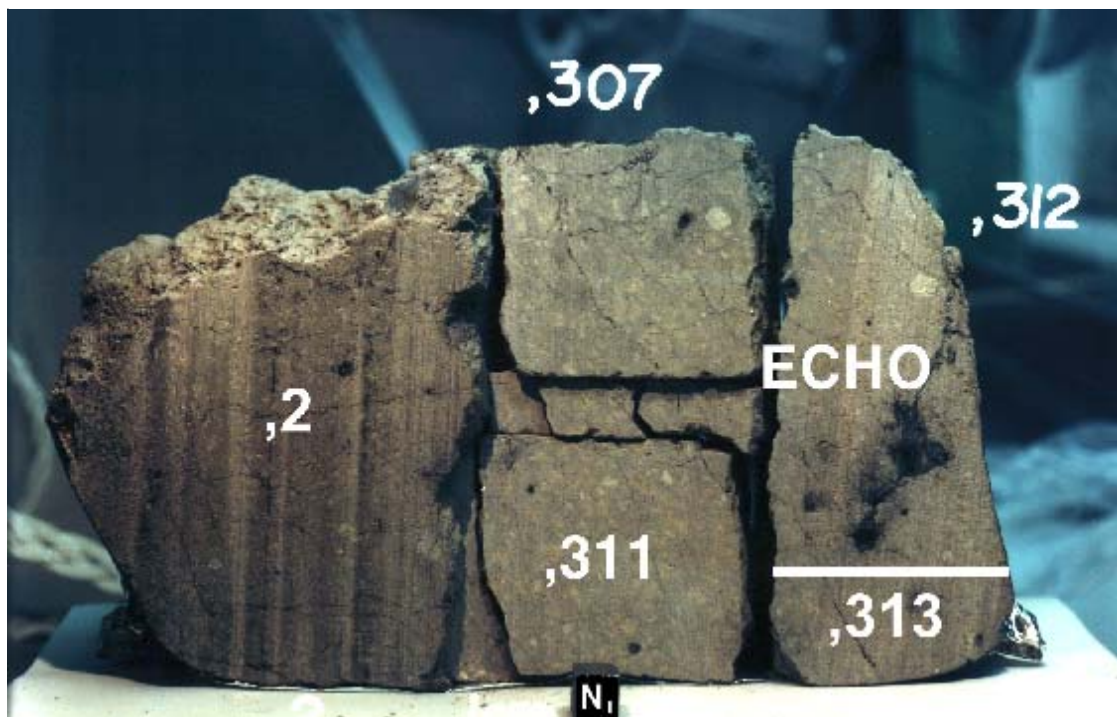


Figure 29. Group photo of EETA79001,2 after the second saw cut showing additional cuts made in 1990. (NASA # S90-34035). Cube is 1 cm (for scale). See exploded parts diagram, figure 22.

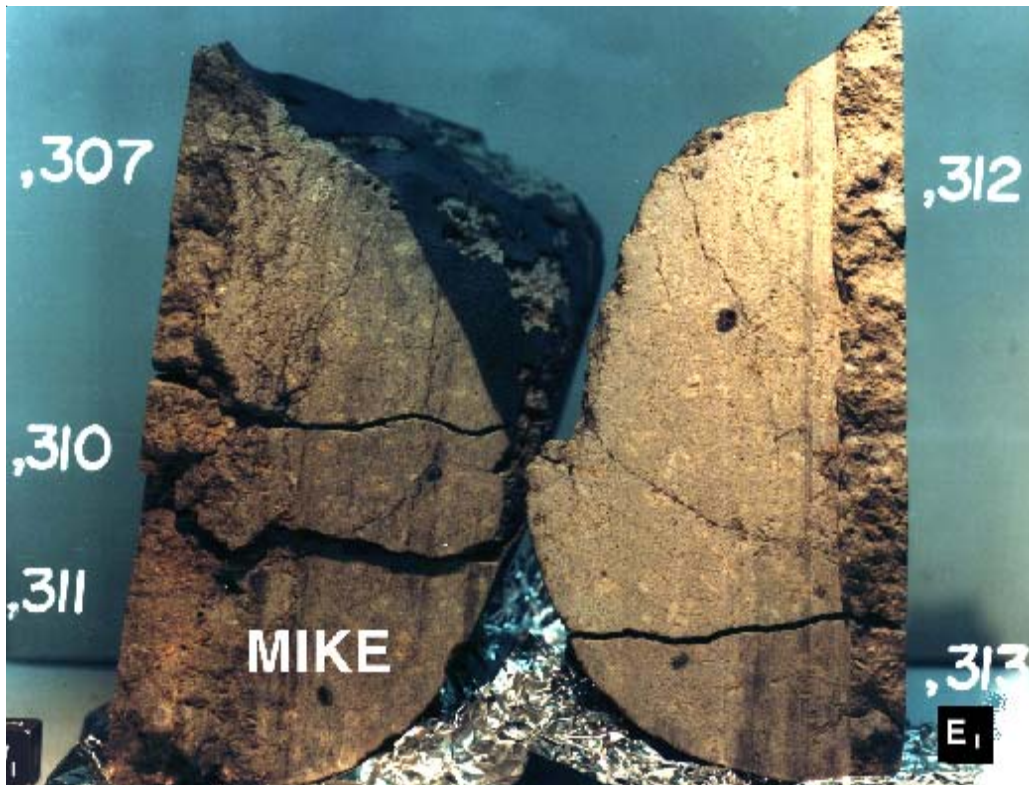


Figure 30. Sawn face of EETA79001 showing opposing pieces. Note the thin glass veins and small glass pods. NASA photo # S90-34042.

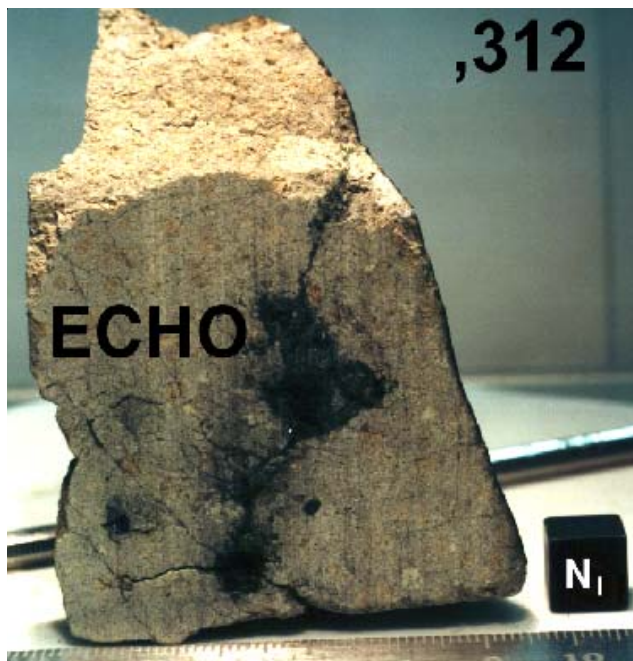


Figure 31. Close-up of glass inclusion (ECHO) and interconnecting glass veins and cracks. (NASA #93-33193).

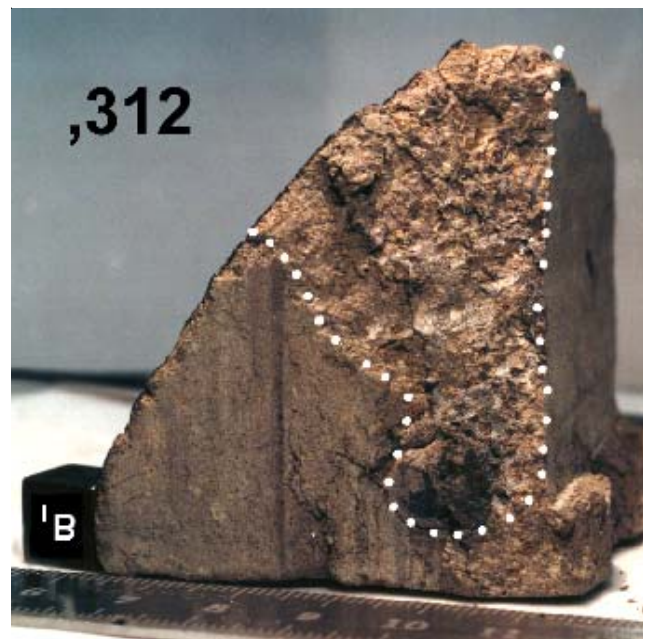


Figure 32. Close-up photo of area sampled for "druse" along fracture in EETA79001,312. This sample (363) was used to search for amino acids. (NASA # S93-33190).

EETA79001 Lithology C

(distinct glass pods, most in lithology A)

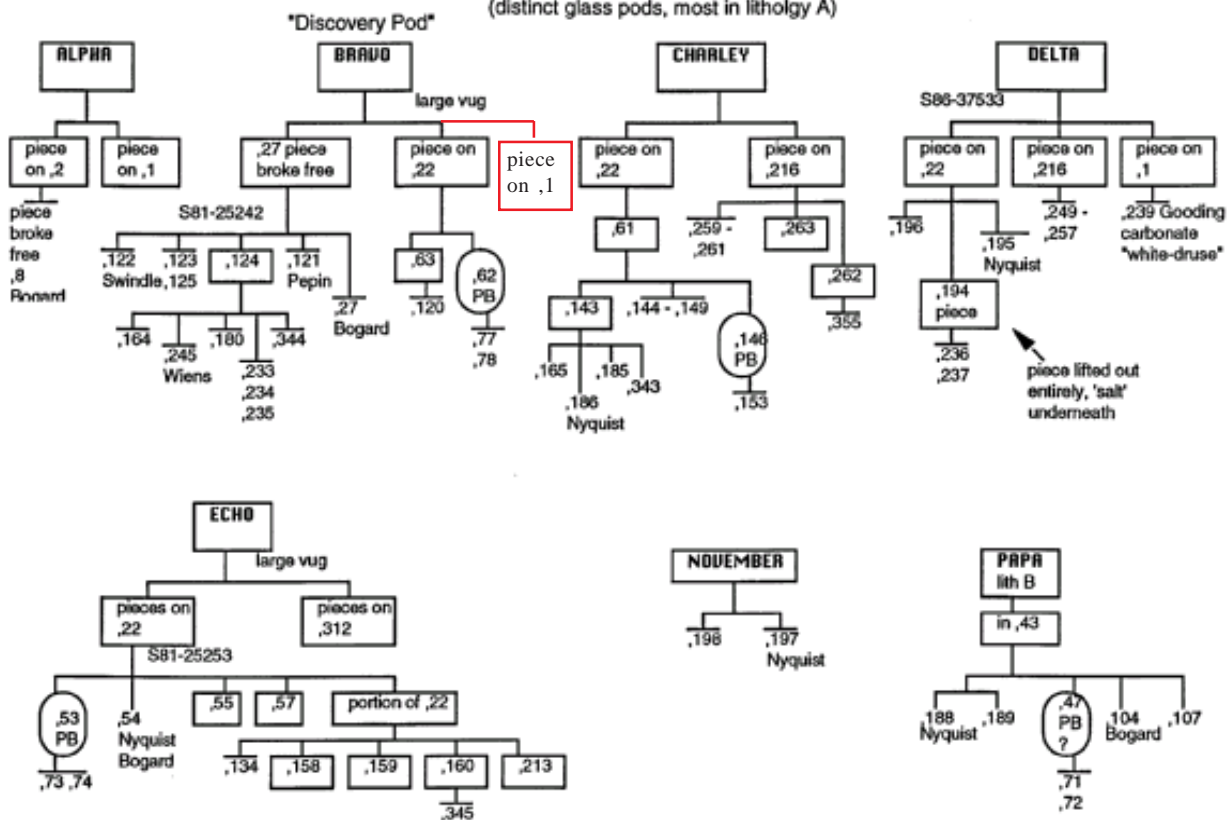
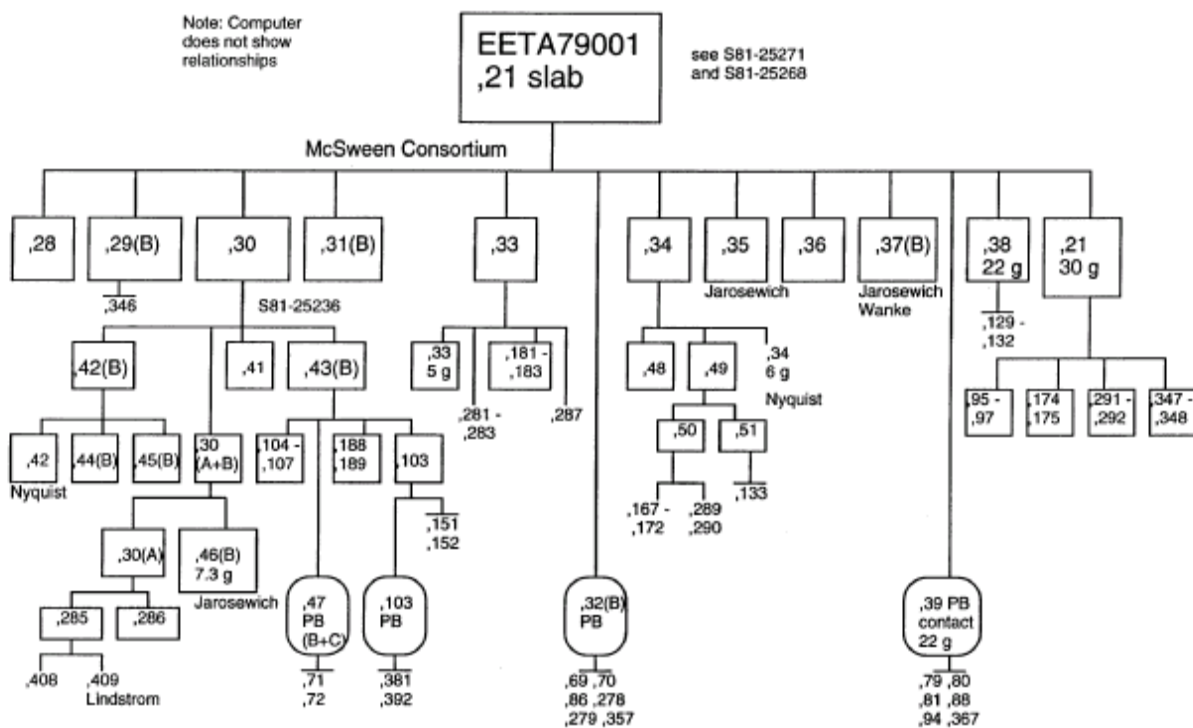


Figure 35. Genealogy diagram for lithology C (the glass pods) of EETA79001.



C Meyer 1996

Figure 36. Partial genealogy diagram for EETA79001,21 (consortium slab). See also figure 24.

big pieces only 2012

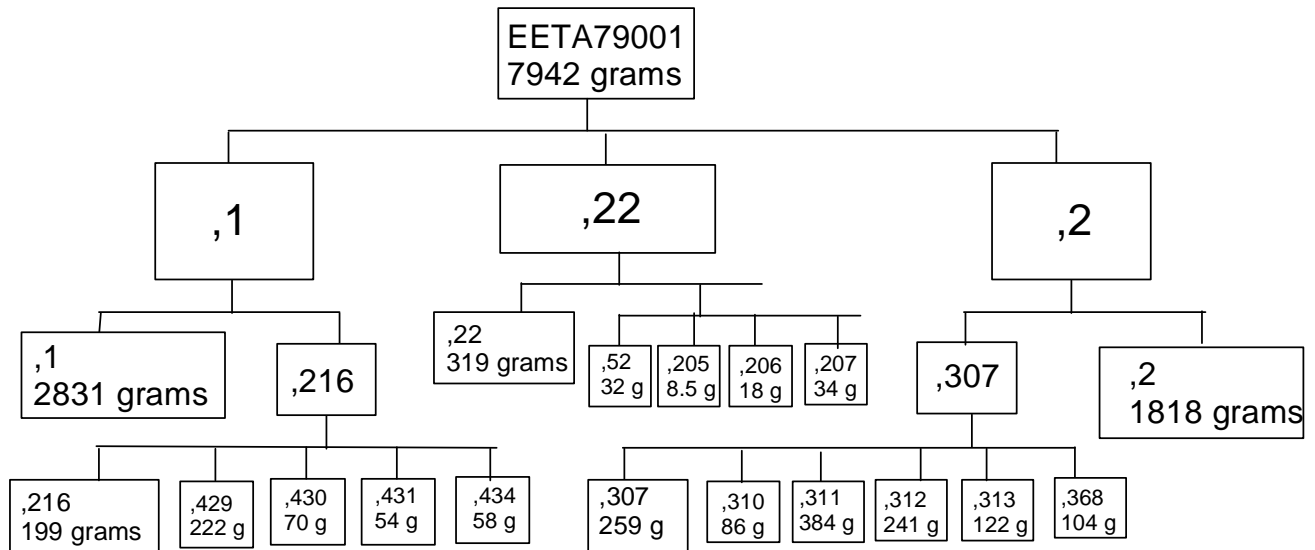


Figure 37: Diagram showing the relationship of the largest pieces of EETA79001 as they exist in 2012.

Salisbury *et al.* (1991), Hamilton *et al.* (1997) and Bishop and Hamilton (2001) have determined the reflectance spectra of EETA79001. Raman spectra of various minerals in EETA79001 have been determined by Wang *et al.* (2000, 2001).

Processing

The processing of EETA79001 has proceeded along the lines of a 3D jigsaw puzzle (figures 21 and 22). In 1980, a slab was cut from the center of the meteorite, along the long dimension of the rock, creating two large pieces (,1 and ,2) and a cm thick slab that broke into two pieces (,21 and ,22). Most initial allocations were made from these slab pieces (figure 24). In 1986, a third cut was made perpendicular to the 1980 cuts, dividing ,1 into two pieces (the big piece ,1 and ,216). Lithological maps of these sawn surfaces are figure 25 (Martinez and Gooding 1986). In 1990, the remaining large piece (,2) was further cut to create three pieces (big piece ,2, middle piece ,307, and end piece ,312). A small slab ,310 was created from the center of ,307 leaving end pieces ,307 and ,311. Piece ,313 was also cut from ,312 and adjacent to ,311. Adjacent samples ,311 and ,313 (end pieces with fusion crust) were sent to the Smithsonian (USNM) for public display. The remainder of ,307 was allocated to NASA as a display specimen.

This sample was the subject of a consortium led by Hap McSween (see McSween and Jarosewich 1983; McSween 1985). In 1980, homogenized powders were

prepared by Jarosewich of both lithology A (15g) and B (9g) (see Jarosewich 1990b). Splits from these powders are available to investigators by request to MWG.

Lithology B (~400 grams) was located at one end of the specimen and is now on pieces ,1 ,2 ,216 and slab piece ,21 (figure 23).

Lithology C is represented by many different glass “pods” (table 1, figures 26 to 31) and thin glass veins. Sample ,27 (BRAVO) is the large glass inclusions (lithology C) where the evidence of trapped Martian atmosphere was first found (see figure 5). The first saw cut went right through this glass inclusion leaving a portion of it attached to ,1. It contained a large glass-lined vug. Much of sample ,27 later broke free from the boundary of slabs ,21 and ,22. Glass inclusion ,8 (ALPHA) which also broke free during initial processing, has now been studied by Garrison and Bogard (1998). *However, as of 2012, these glass “pods” have not been properly studied and the critical mineralogic and textural data is lacking.*

EETA79001 has been frequently broken-up for allocations; there are now well over 500 splits! In order to provide some clarity to the allocation of this large sample, figures 33 and 36 of the various splits are provided. Figure 37 is provided as an update on the largest pieces as of 2012. However, these diagrams are not complete and one must refer to the meteorite

data base at JSC (MRP). The NASA-Smithsonian Educational Thin Section sets include EETA79001 (French *et al.* 1990).

Please note that the orientation cube in photos taken in 1990 and 1993 was placed in the wrong orientation (reversed).

Lithologies B and C are listed as “restricted” samples by the MWG (Score and Lindstrom 1993, page 5), which means they are allocated and processed with extra-special care.

Note: Since this compiler finds that he is confused about this rock, it would seem that it again needs to be studied in “consortium mode” (with particular attention to the hypothesis that it has incorporated Martian soil – both as “pods” and as dissolved material in the basaltic portion).

References for EETA79001

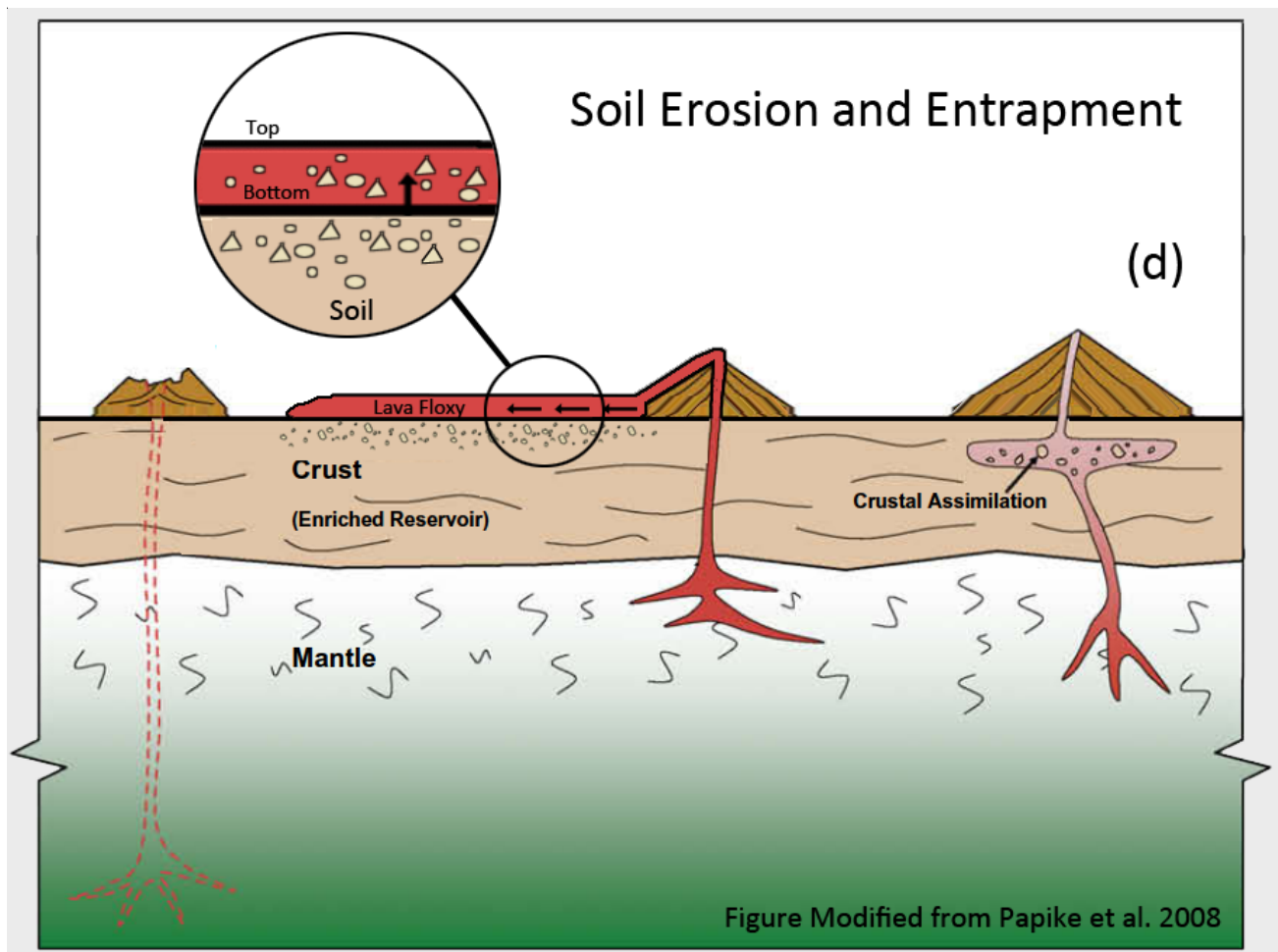


Figure 38: Cartoon illustrating hypothesis 3 (see text). It seems entirely reasonable that 200-500 m.y. old Martian lava flows have eroded ancient irradiated Martian soil and become contaminated and oxidized in the process. Insert depicts how lithology B and C became entrapped in lithology A. However, while soil contamination would explain some features of shergottites (such as variable oxidation state, excess Ar etc.), it would not seem to explain the general trends that so many people have worked hard to decipher (see review by Papike *et al.* 2009). In any case EETA79001 seems to have caught this process in action (see pictures of slabs in this section).